Cape Peninsula
University of Technology

SIMULATION OF A MULTI-STAGE FORMING PROCESS TO INVESTIGATE FAILURE IN THE FORMED PART

By: Nicholas Sandisile Goniwe

Dissertation submitted in fulfilment of the requirements for the degree and counting towards 50% of the final mark

Master of Technology: Mechanical Engineering

in the Faculty of Engineering at the Cape Peninsula University of Technology

Supervisor: Prof G J Oliver

Bellville: December 2016

DECLARATION

I, Nicholas Sandisile Goniwe, declare that the contents of this dissertation/thesis represent my own unaided work, and that the dissertation/thesis has not previously been submitted for academic examination towards any qualification. Furthermore, it represents my own opinions and not necessarily those of the Cape Peninsula University of Technology.

Signed **Date**

ABSTRACT

The purpose of this study is the optimisation of the stamping analysis process in order to investigate the possible reasons for the part failure. (Altan & Vasquez, 2000) have conducted similar research to optimise a forming process. However, they focussed on dies for a forging process and in this study, we are looking at cold forming and this study is also different in that we are trying to reduce the number of stages while maintaining the formability. Formability is based on the dimensional conformance of the final part with additional criteria being the thinning, appearance of wrinkling, dynamic effects leading to the localisation of strain, cracking and residual stress. A numerical modelling procedure that is close enough to the real process is used to investigate the effects of changes in the frictional contact that would correspond to lubrication and also the effect of adding draw beads to the forming tools to change the frictional contact. We also investigated the effect of using a different material in terms of meeting the design requirements.

Experimental results for comparison are available for certain of the stamping processes investigated that were tested in pre-production. The finite element simulation is used to account for all residual thinning, stress and strain of the multi-stage forming process to ensure optimum thickness changes of the sheet at each stage. The variations of material and manufacturing parameters are established to accurately predict the behaviour of this specific forming process. The material model required to meet physical experiments is deduced from the results of standard tensile tests and fitted to the Hill's 48 Law for Work Hardening. The commercial packages Ls-Dyna with Dynaform and Pam-Stamp software are used for the simulation to produce 2 results for comparison.

The simulation setup of each stage was defined using a number of predefined operations namely: preforming, forming, re-striking and flanging and springback. The simulation setup for at each of the stages was carried out taking into account spring-back. The optimum tool shapes with thickness changes at each stage were found using the results of the previous operation.

The first simulation of the process, the blank was clamped in a fixed position by the blank holder against the punch to perform preforming. With the movement of the punch, the material was pushed over the forming die. The forming and striking of the blank are done on the second and third stage. Then, the blank is transferred from the forming stage to the flanging die stage. The flanging die stage was designed to compensate for

the parameter changes of the blank after the end of forming operation. The flanging operation is carried out to make sure that the desired intricate shape is met. The scheme for the numerical simulation of the multi-stage process of the stages decided upon is presented in Figure 10 in sequential order.

The numerical results for a multi-stage forming process were calculated with the tooling setup for the blank size used in pre-production and existing process parameters that were tested. The result as discussed in chapter 7 indicates that after the second forming stage the Von Mises stress reaches a maximum in the area near the angled surface walls where the greatest thickening occurs.

The highest stress concentrations are found in the areas where the forming originally developed in the forming process. The areas where the high stress prevailed after forming were those in which the angle of bend change abruptly to the region of 85º-90º had the maximum springback deformation. The springback causes a loss in overall accuracy of the finite element results in terms of conforming to the desired shape. The springback magnitude was found to be in the region of 0.4 -1.09mm. This exceeds the tolerance with respect to the final desired part of 0±0.8mm.

A 5-stage forming process was successfully simulated. A number of material and process parameters had to be input into the explicit dynamic finite element analysis with contact and friction which makes this analysis more complex than, for example, static structural analyses. The results produced show an agreement with the desired shape. A maximum residual stress is predicted for the final product.

The simulation process can be repeated for different tooling and process parameters to arrive at an acceptable finished part without having to physically manufacture the tooling. Future work in relation to this optimisation framework includes the attempt to reduce the number of forming stages and investigation of the dimensional conformance of the part for different material choices.

ACKNOWLEDGEMENTS

I would like to express my sincere gratitude to my supervisor, Professor Graeme Oliver for his support during the course of M-Tech study. Your willingness to transfer scientific knowledge has been greatly appreciated.

I would also like to thank our industrial partner, Precision Press, for permitting us to use their data for this study. Barend Burger has been very helpful and his understanding of nature technical challenges has made it possible to complete this study.

I am so grateful to the Institute for Advanced Tooling for availing their state-of-the-art equipment and my colleagues for their technical contribution and support.

The support and understanding of my family during lonely times has been amazing, thank you so much.

Most importantly, biggest thanks to my mother, Noluthando Goniwe for her guidance and the strong believe in education, without your support I would not have been acknowledging you in this thesis, in fact, I would not have progressed to the tertiary level, thanks, Tyhopho.

Lastly, the financial assistance of the National Research Foundation and the Cape Peninsula University of Technology towards this research is acknowledged. Opinions expressed in this thesis and the conclusions arrived at, are those of the author, and are not necessarily to be attributed to the National Research Foundation.

TABLE OF CONTENTS

LIST OF FIGURES

LIST OF TABLES

1. INTRODUCTION TO MULTISTAGE SHEET-METAL FORMING

1.1. Multistage sheet-metal forming

It is one of the major fabrication processes in the automobile and aerospace industry which typically includes multi-stage sheet-metal forming, such as blanking, drawing, sizing, trimming, etc. Multi-stage is a process of sequentially forming a metal sheet through various shapes from plane sheet to the desired shape of the component. The process of determining the number of stages required to form the component without failure takes years of experience. It is a common practice in the tool and die making industry, especial in sheet metal forming operations.

The dies required should be optimised to account for the changes of the process parameters at each stage to ensure the forming quality. Through the years, technology advances have allowed the production of extremely complex parts.

The number of stages required to obtain the final shape of the product is always not known for sure at the start of the tool development. However, the dedicated CAD/CAE sheet metal packages make it possible to streamline the entire die making process required for the die development.

1.2. Motivation and objectives

The main objective of this study is the optimisation of the stamping analysis process in order to investigate the possible reasons for the part failure. The process will demonstrate the simulation of different stages of stamping operation and so to illustrate the advantages achievable in the conceptualisation phase of the tool design. This process will try to influence strategies to develop key aspects of tool development such as:

- develop a method to optimise the tool design concept in the beginning of the tool development to ensure that the tool cost remain competitive
- guide multi-stage practice and physical simulation and forwarding the use of advanced manufacture technology in the sheet metal forming industry in South Africa

This will, hopefully, make the design process smoother and also spare the company expensive trial and error time. Also, after the project, a company can, at least, qualitatively evaluate if an advanced simulation tool would be profitable.

1.3. Problem statement

The case study depicted in Figure 1&2 is an automotive component used in a catalytic converter system. This component is produced by Precision Press Company, a metal pressing company in the Western Cape, South Africa. The component is formed by a fourteen stage progressive tool due to the complex geometry.

Figure 1: Case study - (SAMPLE) automotive component

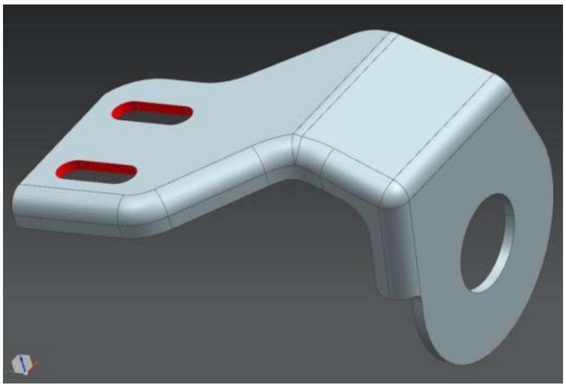

Figure 2: Case study – (MODEL) automotive component

However, it is formed with physical defects on the flanged wall where two angled surfaces meet. During the Photovoltaic (PV) hot vibration test, the component shows apparent micro cracks in the region with physical thickness variation. Figure 3 shows compressed material with local thickness variation. The material is compressed and shows local thickness increase on a large area of the flanged wall.

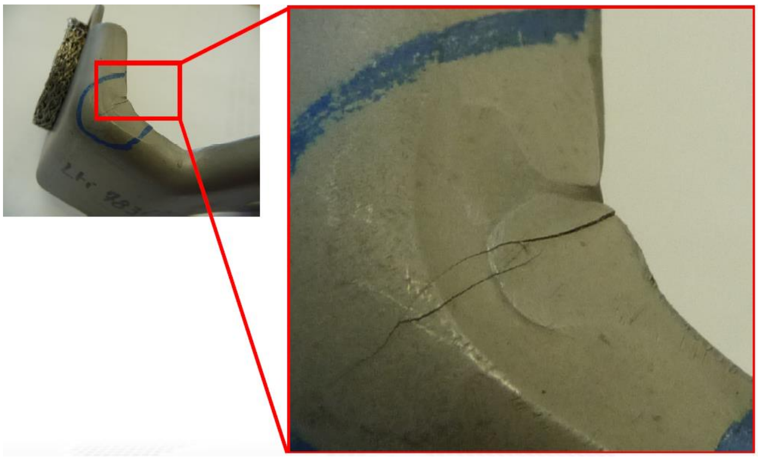

Figure 3: Component with local thickness increase and micro crack

1.4. Scope of the study

The study will focus mainly on the investigation of the cause of micro crack near the two angled walls of the flanged area as depicted in Figure 3. The trial and error method of determining the number of forming stages required to successfully form the part without failures will not be attended because the tool currently run pre-production. Instead, existing parameters will be used to duplicate the current thickening in the production of forming process with 3mm SUPRAFORM TM380 blank material.

Thereafter, the tooling will be optimised in order to obtain the component quality as per design requirements. This will be done by simulating the forming process with Finite Element Analysis (FEA) package. The package will also be used to analyse the multistage process to account for residual stress between stages of the forming process.

Furthermore, we will compare the measurements of where the crack initiated on the part to what is predicted by the finite element simulation. It will further discuss the results obtained from the production shop on the cause of apparent micro cracking initiated at the location of thickened areas of the formed part.

1.5. Literature review

The purpose of this study is the optimisation of the stamping analysis process in order to investigate the possible reasons for the part failure. (Altan & Vasquez, 2000) have conducted similar research to optimise a forming process. However, they focussed on dies for a forging process and in this study, we are looking at cold forming. This study is also different in that we are trying to reduce the number of stages while maintaining the formability.

Multi-stage sheet metal forming process experience complex deformation which easily results in deformation defects such as fracture, wrinkling, and etc. Previous studies on multi-stage forming process only considered deformation amount of each stage and formability through safety criterion, using strain distribution method (De-hua, et al., 2010). The method does not consider deformation defects while accounting for the relationship between strains of different stages.

(Kurra & Srinivasa, 2014), analysed formability of varying wall angles that can be formed without fracture and assessed the forming limit curve by forming pyramids and conical shapes with different materials. They observed that the maximum error in limiting wall angle prediction with conical and pyramidal frustums was found to be 3.62% and 2.65% respectively.

Further study on formability mechanism was analysed by (Fang, et al., 2014) to describe the localised deformation mechanism taking into consideration of both bending effect and strain hardening. The same study reveals that fracture tends to appear in the transitional zone between the contact area and the formed wall. This suggests that the process development should take careful consideration of deformation that occurs near formed angled wall.

(Fang, et al., 2014), (He, et al., 2013)and (Gang, et al., 2012) have discussed the influence of the constitutive model (hardening law) and yield criterion using comparative analysis between stress and strain based forming limit diagrams. The constitutive models are commonly used to accurately define the hardening behaviour of sheet metals. There has been a lot of work done on the development of constitutive models in the past decades. But a suitable model to match the hardening behaviour requirements of the material used in this study will be adopted accordingly.

The impact of constitutive model and yield criterion of materials has a significant influence on stress calculation (Aghaie-khafri, et al., 2002). Hence, the constitutive model plays an important role in understanding the material deformation behaviour during sheet metal forming process in order to meet the design requirements.

The other factors that contribute to successful forming operations include the coefficient of friction between blank and tooling. The selection of suitable friction data influences the performance behaviour of material for a given operation at different temperatures. (Jayahari, et al., 2012) analysed formability of various materials and evaluation of friction for Aluminium at different temperature conditions. He observed that the prediction of friction becomes complex as its value increases with temperature.

Many materials models have been used in the metal forming process to study the behaviour of the material during simulation. However, most metal forming process has been solved by two approaches – Eulerian and updated Lagrangian formulation (Dixit, et al., 2011). The selection of suitable material model is very important in order to predict the capability and accuracy of the numerical results. Therefore, the selection of a material model that meets the various parameters of the material used will be highly considered for this study. However, there is no clear guideline as to which material model is suitable for a particular material and specific process condition (Dixit, et al., 2011).

Contributing to the fact that the strain deformation method does not consider the deformation defects, this study will investigate the possible reasons for the part failure near the formed angle wall in relation to the conformity of the required part. The amount of residual stress relationship between different stages will be analysed.

1.6. Research design and methodology

A numerical solution will be used to simulate the multi-stage forming process. The commercial finite element based package LSDYNA will be used to produce the numerical solution for the displacement using a metal plasticity model, frictional contact and the current geometry of the forming tools and blank material. An elastic-plastic model will be used to relate the strain field to the stress. The elastic material parameters, Young's modulus and Poisson's ratio, will be for TM380 steel and the plasticity model will include work hardening.

The numerical solution obtained for the displacement of the formed part will allow us to compare the conformity of the part to the required design. The residual stress in the formed part will be measured using the hole drilling method.

The finite element model will be adjusted in terms of material model and frictional contact if there is a mismatch between the physical part and the part predicted by the simulation. Once we have obtained a numerical modelling procedure that is close enough to the real process we will investigate the effects of changes in the frictional contact that would correspond to lubrication and also the effect of adding draw beads to the forming tools to change the frictional contact. We will also investigate the effect of using a different material such as HR190 in terms of meeting the design requirements.

2. OVERVIEW OF THE METAL FORMING PROCESS

2.1. The method used to design the part

The increase in complexity of formed parts has made it even more difficult to estimate the number of stages required to obtain the final shape of the product. Therefore, a strategic die development approach is required for early identification of design errors. The die development framework illustrated in Figure 4 is used to streamline the whole die making process.

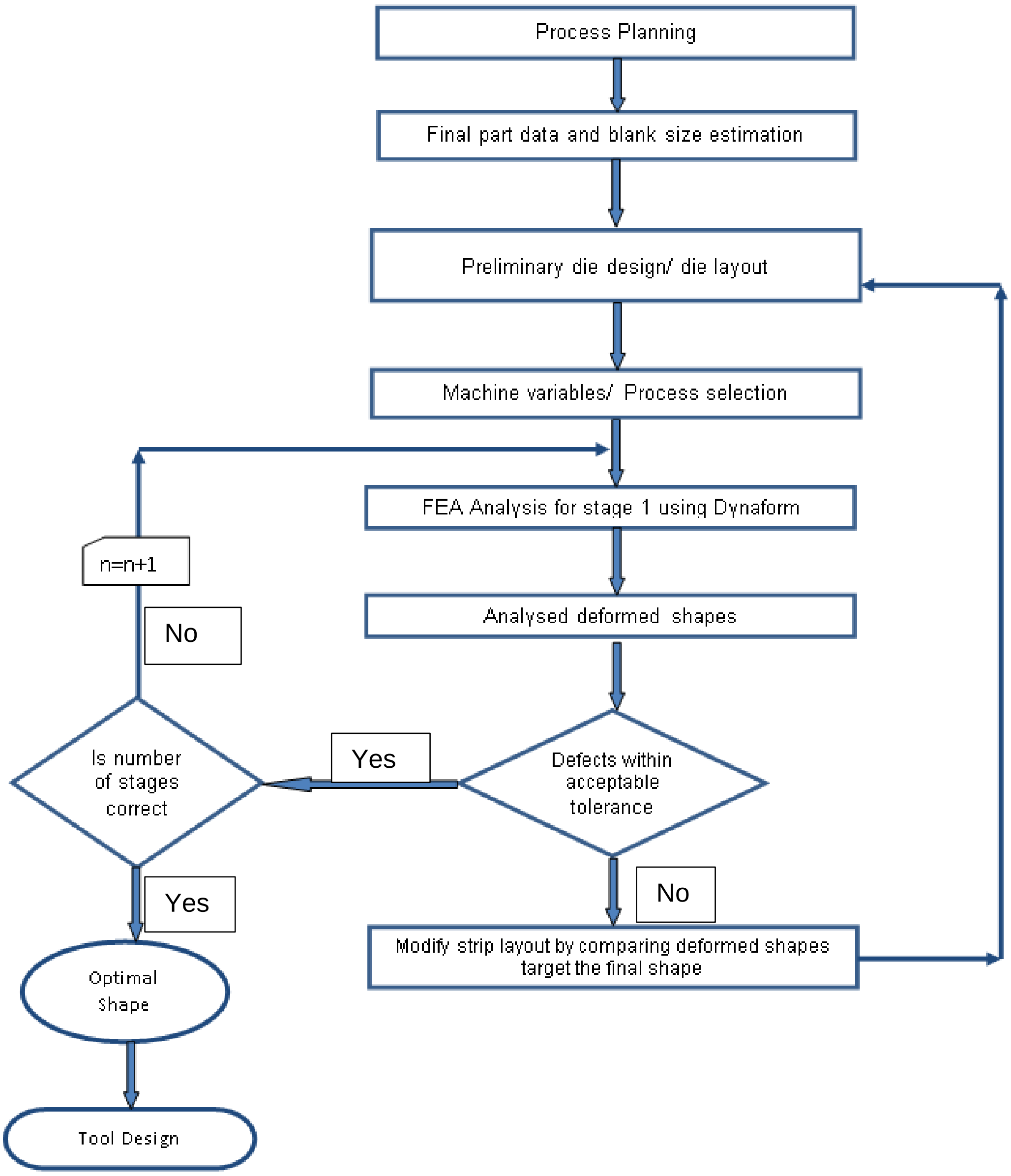

Figure 4: Proposed die design process chain

2.2. Process planning

The initial planning of the die design is based on the knowledge of the final shape of the part to be formed. To a large extent, most companies use their internal guidelines for designing the process sequence which is based on experience. There is little quantitative design information available in the technical literature (Altan & Vasquez, 2000). In order to carry out adequate planning process of the die design, it is necessary to consider in detail the fundamental reasons for selecting a given design, such as the following (Tisza, et al., 2008):

- Part complexity
- Machine parameters
- Type of die
- Material
- Batch size
- Product lifespan
- Anticipated cycle time
- Product tolerances
- Project lead time
- Project budget

In this way, generic answers are provided to guide the designer to determine the customer's precise requirements and also guide the designer in avoiding elementary mistakes.

2.3. Final part data and blank size estimation

Once the process planning has been verified, the optimal blank size is developed based on the prior knowledge of the final shape of the part. This process takes into consideration the material properties of the part to be formed. This optimisation process is based on the trial and error method owing to complex nature of the material and inherent characteristics of metal forming process variables like tool shapes, punch lubrication, blank holder force, and punch speed (Goel, 2004). The example of a blank size estimation is displayed in Figure 5. This is a method of unfolding a final shape of the part into a flat blank outline.

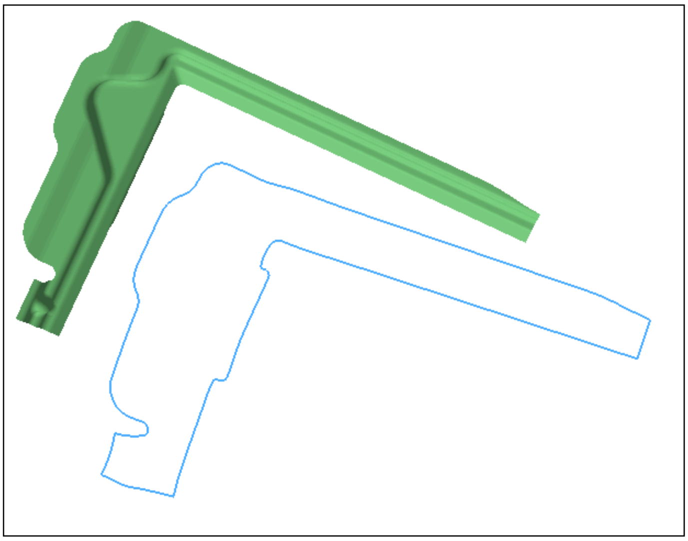

Figure 5: Illustration of blank size estimation

2.4. Preliminary die design/ die layout

This stage involved in the development of the die layout with clear consideration of the following:

- Material requirements and utilisation
- Number of stations (if is a progression die)
- Pitch
- Strip with, etc.

The best location of the sheet blanks is as well important to serve good bending requirements. The grain direction has a huge influence on the quality of the bending operation. When sheet metal is rolled in the steel mill, a fibre, or grain, is produced in the direction of rolling. To obtain maximum strength from bent parts, the bends should be made at an angle of 90° to the grain direction. (See Figure 6 for more details). When the strips are sheared from sheet stock, it is possible that the grain direction may be 90° to the edge of the strip, depending upon how the strip is sheared from the sheet.

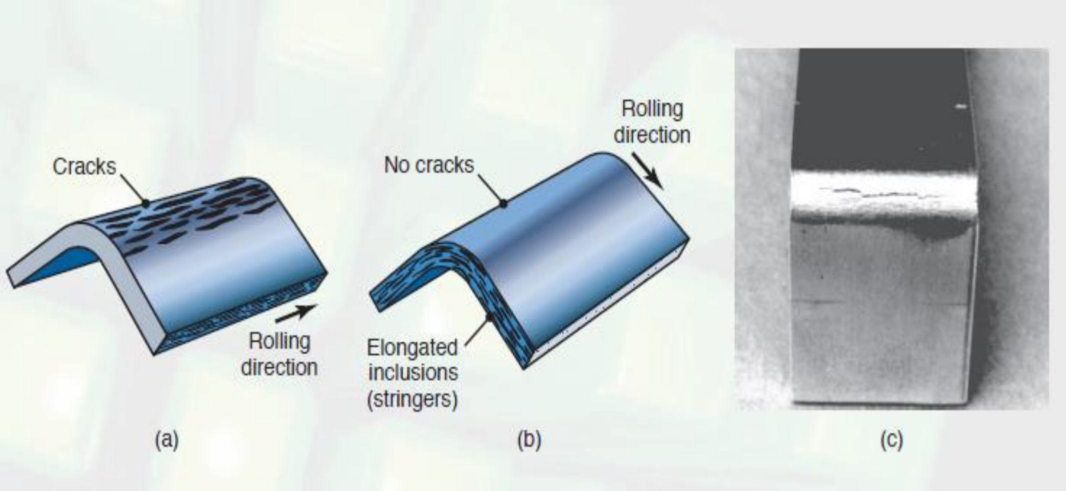

Figure 6: Schematic representation of the effect of grain direction vs. bendability (Schimid, 2008)

Design problems can occur due to many factors that influence the material flow and the geometry. Therefore, the designer has to take into consideration all the factors that may cause unacceptable cost or quality of the formed parts before manufacturing the die. The die layout with an operational description for easy viewing of each stage of the layout is shown in Figure 7 as an example.

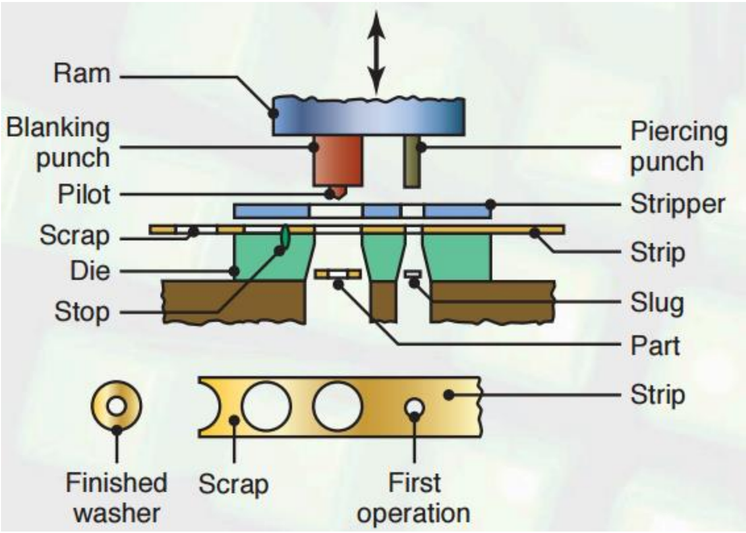

Figure 7: Die layout view of each station on the strip

(Schimid, 2008)

2.5. Machine variables

The die designer must know certain fundamentals of press operation before s/he can successfully design press tooling. Generally, the proper selection of machine press is associated with the kind of die tools to be provided. Figure 8 shows a hydraulic press machine applicable for this forming analysis. While selecting a machine press the following points should be considered (Nagpal, 2004).

- Force required to cut the metal
- Size and type of the die
  - Stroke length
  - Method of feeding and size of the sheet blank
  - Shut height
  - Type of operation

Figure 8: 702 Press Machine from Precision Press

The hydraulic press machine specifications are shown in Table 1.

Table 1: Hydraulic Press machine Specification

VARIABLE	SPECIFICATION
Table size	1.110 – 1.070 mm
T-Slot width	21 mm Top (Ram) – 16 mm Bottom (Machine bed)
Distances between T-slots centres	230 mm Top (Ram) - 212 mm Bottom (Machine bed)
Stroke	200 mm
Minimum shut height	230 mm
Press speed	50 strokes/min

3. LS-DYNA with DYNAFORM AND PAM-STAMP

The numerical simulation is conducted with two commercial finite element analysis (FEA) software codes, namely Ls-Dyna with Dynaform and Pam-Stamp. The FEA codes have been used to study deformation behaviour of the reference part. The simulation capabilities of the software were not conducted as it was not part of the scope. However, the simulation results of both software are compared with physical experiments.

3.1. Ls-Dyna with Dynaform

The Dynaform software package which uses Ls-Dyna as its solver to perform the FE simulations was used to conduct the simulation. Dynaform is a finite element package using a dynamic continuum formulation specifically designed for forming applications. As such it has material models specifically chosen for sheet metal forming as well as additional non-standard outputs such as the formability and the thinning measures that are not found in standard finite element packages that are capable of analysing dynamic problems (ETA/DYNAFORM, 2006).

3.2. Pam-Stamp

Pam-Stamp is the explicit dynamic finite element method (FEM) with a complete solution for stamping engineering. The simulation package includes explicit and implicit solver technology that enables fast and accurate stamping and springback predictions (PAM-STAMP, 2015).

4. DYNAMIC FINITE ELEMENT ANALYSIS

4.1. Finite element model

A finite element model of the tooling and blank was developed as shown in Figure 9. The surfaces that define the shape (punch and die) are modelled as rigid surfaces and the sheet metal blank is modelled as a deformable body. The simulation method used to account for the process parameters is transient dynamic finite element analysis.

The experimental scheme of the stamping of a component involves a punch, a die and a blank holder (binder). The blank holder moves downwards to hold the blank against the die in a fixed position until blank holder force is achieved. With the movement of the punch, the sheet material is pushed over the die that provides the formation of the desired shape. The control parameters for the movement of the tools consist of the type of contact between forming tools and blank.

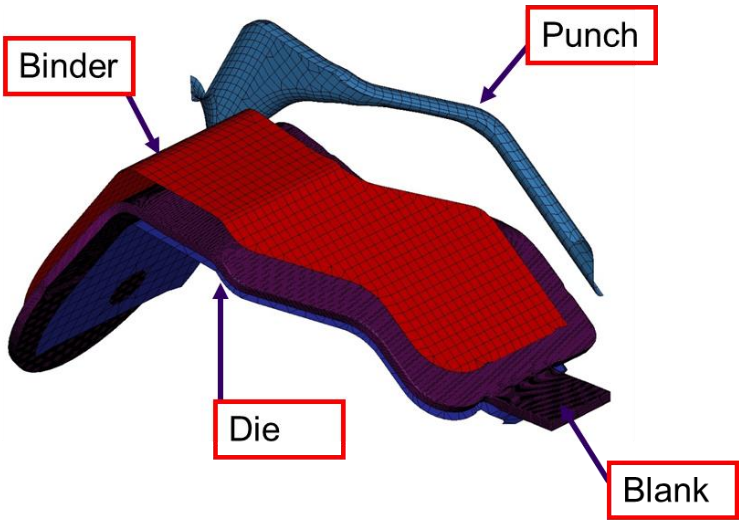

Figure 9: Sheet metal forming operation

4.2. Description of the stamping process

The simulation setup of each stage was defined using a number of predefined operations, namely: crash forming, forming, re-striking, flanging and spring-back. The simulation setup at each of the stages was carried out taking into account spring-back. The optimum tool shapes with thickness changes at each stage were found using the results of the previous operation.

The first simulation of the process, the blank was clamped in a fixed position by the blank holder against the punch to perform crash forming. With the movement of the punch, the material was pushed over the forming die. The forming and re-striking of the blank are done on the second and third stage. Then, the blank is transferred from the forming stage to the flanging die stage. The flanging die stage was designed to compensate for the parameter changes of the blank after the end of forming operation. The flanging operation is carried out to make sure that the desired intricate shape is met. The scheme for the numerical simulation of the multi-stage process of the stages decided upon is presented in Figure 10 in sequential order. A 5 stage process out of 14 stages used in pre-production was decided upon to focus on to make effective use of computational time and in order to observe the dynamic effects leading to the form flanged which has the forming defects.

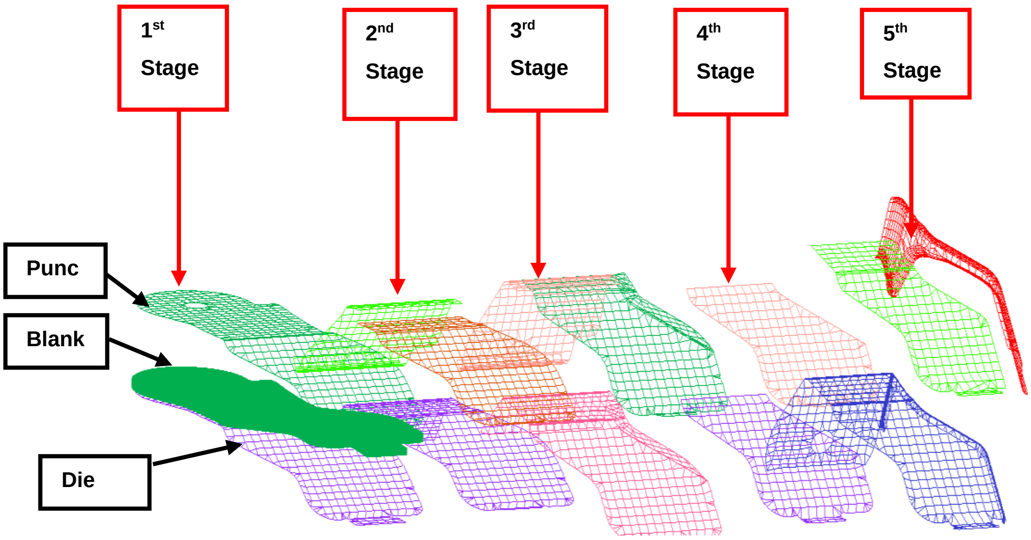

Figure 10: Sheet-metal forming operation divided into five stages: Forming and Flanging

4.3. Computational method used to account for process parameters

The size of the blank material and number of stages needed to obtain the final shape of the part is unknown at the start of the simulation. However, the trial and error method of determining the number of forming stages required to successfully form the part without failures will not be attended for this study because of the tool is in pre-production. Instead, the blank size used in pre-production and existing parameters that were tested will be used to duplicate the physical model with a numerical model.

Formability is based on the dimensional conformance of the final part with additional criteria being the thinning, appearance of wrinkling, dynamic effects leading to the localisation of strain, cracking and residual stress. A numerical modelling procedure that is close enough to the real process is used to investigate the effects of changes in the frictional contact that would correspond to lubrication and also the effect of possible adding draw beads to the forming tools to change the frictional contact. We also investigated the effect of using a different material in terms of meeting the design requirements.

4.4. Mesh used for the simulation

The CAD file needed to be modified to eliminate the overlaps and gaps existing between patches so that the finite-element mesh could be constructed. The tools (blank, punch, die and binder) were meshed separately. Table 2 shows mesh data for feasibility (shell elements) and final setup represented by solid elements.

Table 2: Blank mesh data for feasibility and final setup

MESH DATA		
Part	No of Shell elements	No. of Solid elements
Blank	5799	59910

4.4.1. Shell elements

Shell elements were used to simulate the failure in the part during the forming process. It has been observed that shell elements did not accurately capture the geometry of the model as the mesh was distorted badly next to the predicted fracture region. Figure 11 shows the flat blank mesh with shell elements. It predicted the maximum thickening only at the edge of angled walls of the flanged area while most of the thickening can be found in the bigger area on the pre-production part. These results explain why it was necessary to use solid elements to accurately predict the deformation of the part. Figure 12 illustrates distorted mesh.

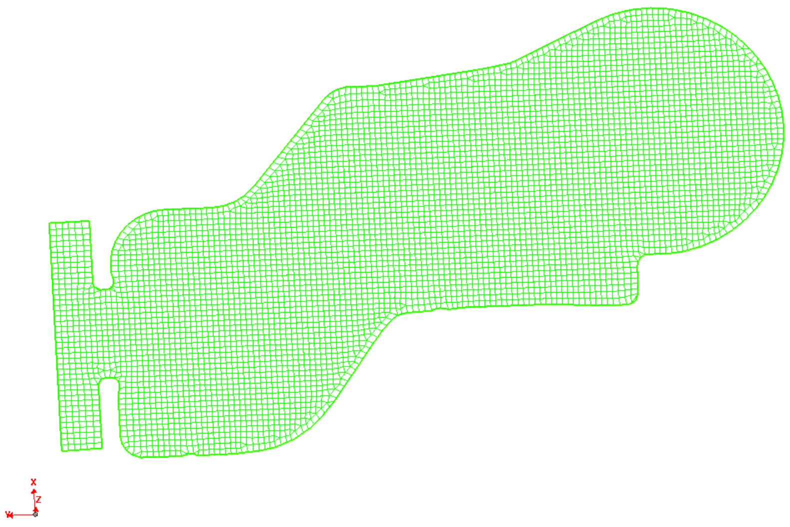

Figure 11: Initial meshed blank with shell elements

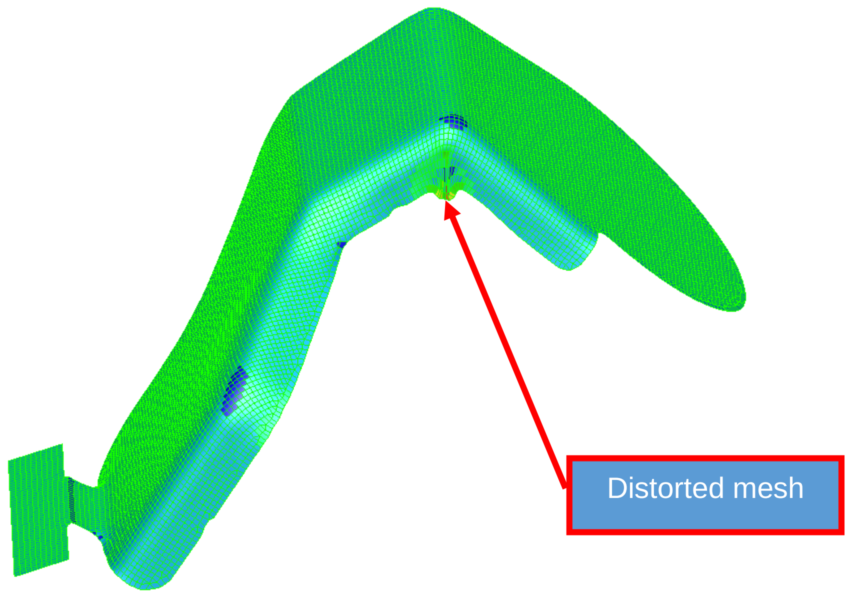

Figure 12: Initial blank with distorted mesh

The blank is initially meshed using a combination of 3-noded triangular and 4-noded quadrilateral shell elements which are shown in Figure 13.

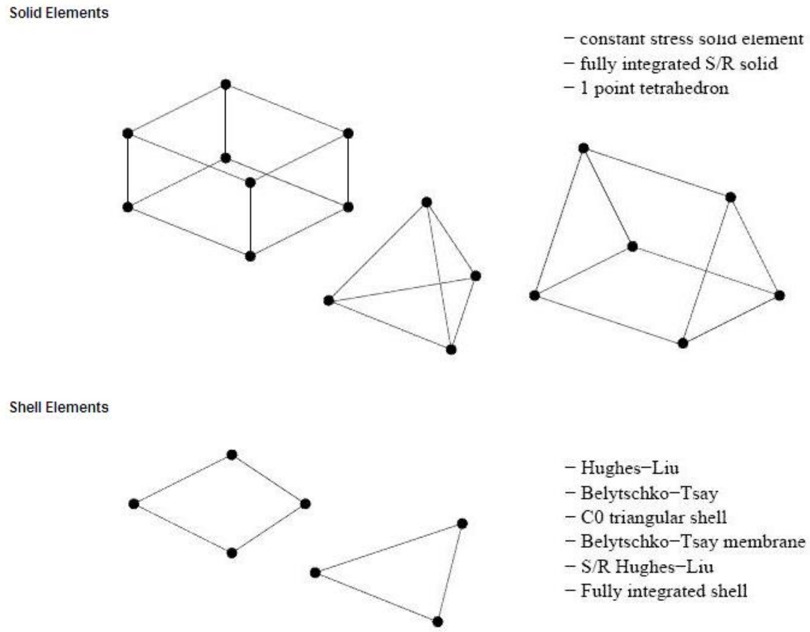

Figure 13: Quadrilateral and triangular shell elements along with other continuum elements used in LS-DYNA (ETA/DYNAFORM, 2006)

The accurate forming simulation requires a very fine mesh in the area of tool radii or curved regions (Hallquist, 2007) and (Park, et al., 2004). Quadrilateral shell elements perform better than triangular shell elements because they can represent a linear variation of stress rather constant stress over the element so the bulk of elements are quadrilateral elements forming a regular mesh with triangular elements only used to conform to the curved radii (Morris, 2008). The blank was meshed with shell elements using full integration with five integration points defined through a thickness of 3 mm. It was determined that the four-node shell elements using full integration with five Gauss integration points through the thickness were required in the blank to correctly capture the plasticity (Park, et al., 2004).

4.4.2. Solid elements

When we perform a simulation we apply some loads and boundary condition to a numerical model of the structure, that approximates the real material behaviour, and we can then study the effects of the forming process of the blank sheet metal. In this particular case, we observed that shell elements are not ideal for this thick component with a radius sharper than the thickness of the blank.

When the radius is sharper than the thickness of the blank the simulation loses accuracy and provides unreliable results, hence the solid mesh was used for the definition of the blank. Figure 14 shows the blank mesh with solid elements.

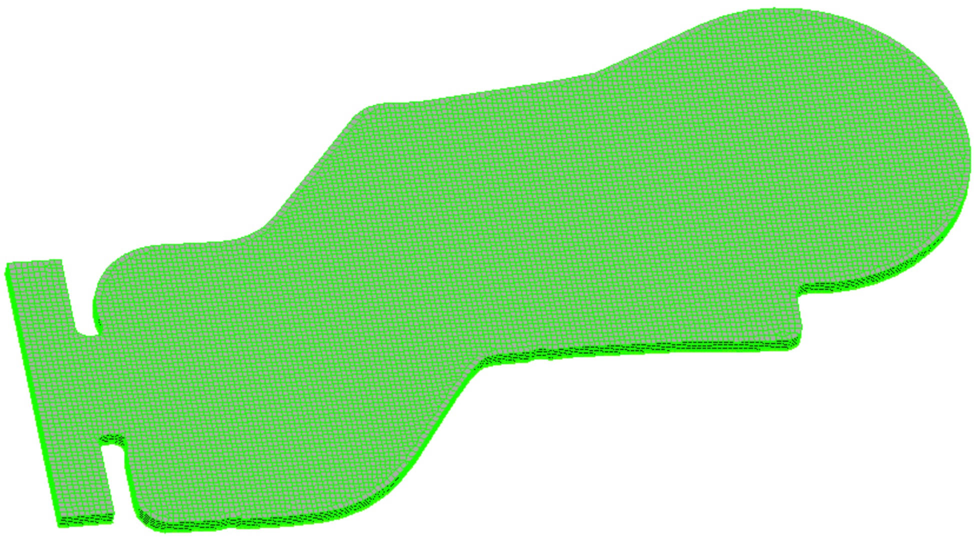

Figure 14: Final meshed blank with solid elements

However, general guidelines mention the length over thickness ratio as a good reference point where the ratio presents a boundary between the choice of shell and solid elements (Wang, 2006). The typical 3D solid mesh is depicted in Figure 15.

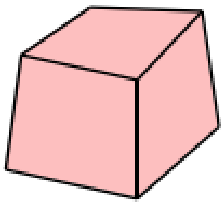

Figure 15: Typical 3D solid mesh

Eight-noded brick elements are used with five integration points. The number of integration points through the thickness is considered to be an important variable. It is mostly used in nonlinear deformation analysis to achieve a good approximation of the material behaviour. (Wang, 2006).

4.5. Contact conditions

The contact options are primarily for treating contact of deformable body to rigid body contact. The surface definition for contact is made up of segments of the shell elements of the surface. Contact was defined between the sheet metal blank and the forming dies. The one-way surface to surface contact as implemented in Ls-Dyna software is used for this simulation. This contact algorithm utilises the penalty forces to limit penetration. This method allows continuous contact of the shell elements. It is highly recommended (Wang, 2006) in stamping simulation with large deformation because the penetration of master nodes through the slave surface is considered in adaptive remeshing.

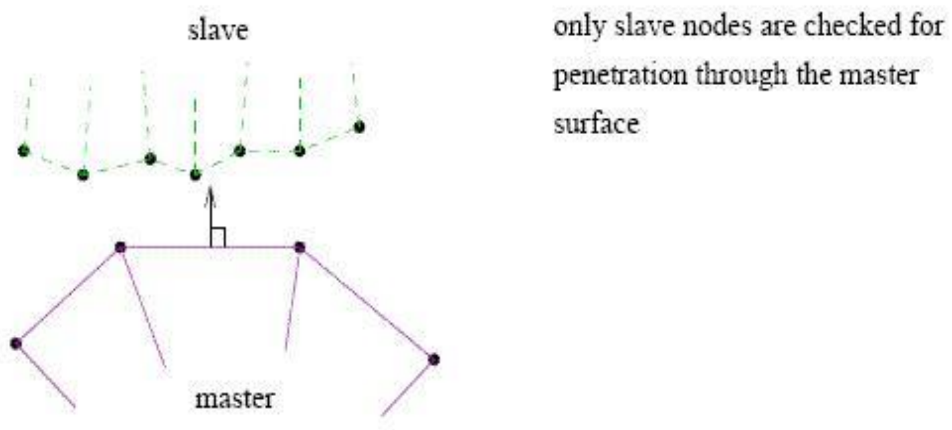

Figure 16: One_way_surface_to_surface contact (Ls-Dyna, 2007)

The slave and master convention terminology are used where one body is designated as the master and the other as slave. Slave nodes are checked for penetration through master segments (See Figure 16).

In the numerical model, an elastic Coulomb friction model was defined with a constant friction coefficient of 0.12 along the die- and punch-blank interfaces, which is the default value in DYNAFORM (Finn, et al., 1995).

4.6. Boundary conditions

The boundary conditions were applied during the sheet metal forming process in order to accurately model the stamping process. The die is completely fixed in all six degrees of freedom: the three translational and three rotational degrees of freedom. The punch was unconstrained only in the direction of the vertical z-axis.

4.7. Blank holder

The blank holder plays a key role in regulating the metal flow by exerting the predefined blank holder force profile. The various values of the binder velocity obtained from pre-production were used to predict the wrinkling and this value is due to change for the series of iterations that will be conducted to optimise geometry. Once these parameters are selected properly, the blank holder profile can eliminate wrinkles and delay fracture in the formed part.

4.8. Springback

Springback is a common phenomenon in sheet metal forming, caused by the elastic redistribution of the internal stresses during unloading. The elastic stress in the bend area after loading is released caused a slight decrease in the bend angle. The metal movement is called springback and the magnitude of the movement varies according to the material type, thickness and hardness (Song, et al., 2007)

Springback has a little effect on the wrinkling and tools force in the sheet metal forming since it happens after removal of the die tools (Song, et al., 2007). The constraints are required to be placed on the blank in order to restrain rigid body motion in the implicit analysis. In this work, the three constraints were applied symmetrically on the flat surface for better inspection of the springback in the centre of the part. These constraints were applied to match the actual forming process. At the end of applying these constraints, the implicit finite element analysis method was directly utilised to determine springback in the component. The results obtained from the implicit solution are outlined in the numerical results.

4.9. Wrinkling

Wrinkling is the phenomenon of compressive instability from the view of mechanic analysis. Excessive metal flow causes wrinkling in the part, while insufficient metal flow will result in fracture, skid marks or splits and thinning (Song, et al., 2007).

Wrinkling affects forming through high values of the blank holder pressure causes higher frictional forces which lead to metal flow restriction. Blank holder pressure should be only high enough to avoid wrinkling tendencies of the metal. If the maximum pressure of the blank holder is more than one-third of the forming force it may affect the metal flow of the blank and result in tearing of the forming wall (Song, et al., 2007).

When forces are become larger, scoring wrinkling and tearing become a problem, a lubricant should be used. These effects are discussed in detail with regards to the numerical results. (Song, et al., 2007)

4.10. Key simulation settings in Ls-Dyna

PART

Parts identification (pid). This part has attributes identified by section identification (sid) and material identification (mid).

SECTION

Parts identified by (sid) are defined by this keyword. Element formulation, integration rule, nodal thicknesses and cross section properties are defined.

MAT

Parts identified by (mid) are defined as a Material Model by a set of parameters.

ELEMENT

Three different element types can be defined: shell, thick shell and solid (brick) elements. Identified by element identification (eid), have the attributes of (pid) and are defined by the node list (nid).

CONTROL_TERMINATION

This control card is used in specifying when the software should stop the simulation calculation. The termination could take place in the form of specifying the termination time, termination cycle, termination mass, the percentage change in energy ratio. A termination time was specified for this simulation.

CONTACT

In LS-DYNA contact is defined by identifying (via parts, part sets, segment sets, or node sets) locations that are to be checked for potential penetration of a slave node through a master segment. The ONE_WAY_SURFACE_TO_SURFACE contact is used for this simulation

INCLUDE

The *INCLUDE keyword provides a means of reading independent input files containing model data. The simulation contains "blk" file and "mod" files.

5. MATERIAL MODEL FOR METAL PLASTICITY

The metal plasticity theory is a method used to describe the plastic behaviour of the materials. The theory assumes that the hydrostatic static pressure has a negligible effect on the material strain hardening and the flow stress is independent of the third deviatoric stress invariant. The main shortcomings of this theory based on localisations (Bai & Wierzbicki, 2007) are the inconsistencies present in the state of stress and strain in the potential fracture. To obtain more accurate simulation results and avoid this deficiency, more recent models have been introduced to improve the accuracy of the material response prediction.

Among these works (Teherizadeh, et al., 2015) presented a model with non-associated plasticity model with anisotropic and nonlinear kinematic hardening. The overall idea is to select a constitutive model that has a possibility to describe the known material characteristically behaviour such as: non-linear, strain-rate-dependent and anisotropic.

Furthermore, reliable forming simulation results of finite element simulation are greatly dependent on the correctness of the input properties and appropriate selection of material models (Kotkunde, et al., 2014). A suitable material model is based on the physical understanding of the ductile fracture phenomenon. In this work, appropriate selection of material model will be implemented based on the match for forming behaviour of the pre-production part used. The material used in practice is SUPRAFORM® TM380 steel.

The focus of this work is mainly in the investigation of the cause of micro crack initiation near the flanged wall; the choice of suitable plasticity model that accurately present the behaviour of the material is vitally important.

The material considered is highly anisotropic, therefore, a selection of yield criterion that provides an accurate prediction of metal plasticity is also essential.

The second material such as HR190 is used to investigate the effect of different material in terms of meeting the design requirements and better formability.

Both materials (SUPRAFORM® TM380 and HR190) present the behaviour of some highly anisotropic high strength material grade. Constitutive model matching the material parameters are discussed in section 5.1

5.1. Constitutive model

5.1.1. Orthotropic Elastoplastic Material Model

In this study, we have defined a material model that matches the parameters of the material used in practice. The input parameters of the TM380 steel were obtained from the tensile test using a specimen to find the behaviour of the material. The input parameters required by this material law include the effective strain-stress curve in a tabular form which describes the hardening curve shown in Figure 17.

The constitutive model used in Pam-Stamp is an orthotropic elastoplastic material model. It allows simplified modelling to address critical material parameters.

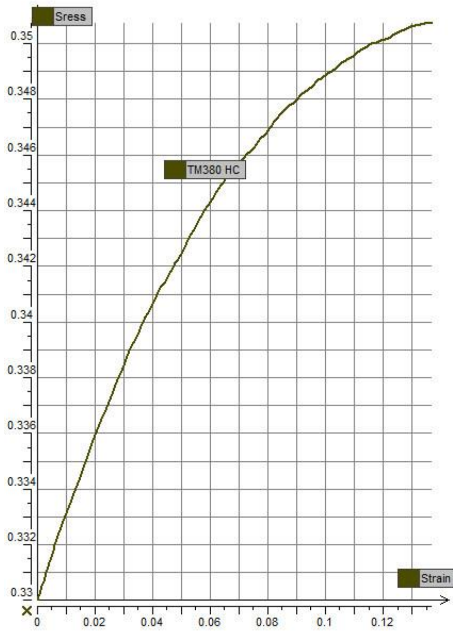

Figure 17: Strain-stress curve for the point list model which corresponds toTM380 steel

The work hardening model for the yield stress used is the Hill 48 yield criterion and is defined as follows (Jan & Miroslav, 2012):

$$\varphi(\sigma_{ij}) = (\sigma_{22} - \sigma_{33})^2 + G\ (\sigma_{33} - \sigma_{11})^2 + H\ (\sigma_{11} - \sigma_{22})^2 + 2L\sigma_{23}^2 + 2M\sigma_{31}^2 + 2N\sigma_{12}^2 - \sigma^{-2} = \pi r^2 = 0 \qquad (1)$$

Where F, G, H, L, M and N are Hill's anisotropic parameters which can be expressed by Lankford's coefficients,

$\sigma_{xy}[MPa] - x, y$ are the principal anisotropic axes.

$$F = \frac{r_0}{r_{90(r_0+1)}}, G = \frac{1}{(r_0+1)}, H = \frac{r_0}{(r_0+1)}, N = \frac{(r_0+r_{90})(1+2r_{45})}{2r_{90(1+r_0)}} \qquad (2)$$

Where, r0, r45 and r90 represent anisotropy are used with effective stress and strain properties in the actual model.

The model allows the use of Lankford parameters for the definition of the anisotropic yield function. The Lankford coefficient is a measure of plastic anisotropy used to characterise a sheet's formability. These anisotropy values are measured in 0º, 45º and 90º to the rolling direction. L and M are equal to N.

This ratio is calculated at different angles as Lankford parameters which allow one to define the anisotropic yield stress as described in the equations which follow (Hallquist, 2007) and (Finn, et al., 1995). (Janbakhsh, et al., 2014)

The initial values for the anisotropic coefficients as measured stress as a function of strain for uniaxial tension in the direction of r0, r45 and r90 are listed in Table 3: Lankford parameters corresponding TM380 material Table 3. These r-values are used with effective stress and strain properties in the actual model.

Table 3: Lankford parameters corresponding TM380 material (Dynamore Support, 2015)

r0	**0.8**
r45	**1.2**
r90	**0.9**

After calculating the corresponding Hill constants using the Equation1 for the effective strain-stress curve, the values for Hill's parameter summarised in Table 4.

Table 4: Hill parameters for given r-values for solid elements

F	**0.49**
G	**0.56**
H	**0.44**
L	**1.78**
M	**1.78**
N	**1.78**

5.2. Material characteristics

The definition of the material in the finite element simulations plays an influential role on the behaviour of the blank material as results of forming. The numerical material model with plasticity model that match the parameters used in pre-production is discussed. Two different material choices (TM380 and HR190) have been used for this study in order to meet the design requirements and better formability. The main material used in pre-production is TM380 which is harder than the HR190. HR190 is a much softer material with improved ductility.

5.2.1. SUPRAFORM® TM380 Steel

The main material is hot rolled high strength, low alloy structural steel with improved formability and good weldability. The material has been developed mainly for applications where pressing, stamping or forming has to be carried out on structural steel. The material is currently produced only as a strip-mill product so that the width is limited to a maximum of 1800 mm. Production parameters impose a minimum thickness of 2mm for the lower and 3mm for the higher-strength grades.

5.2.1.1. Material properties

The material parameters used in the study are given by the South African Arcelor Mittal Steel Corporation which is the producer of the steel. The relevant material properties are listed in Table 5.

Table 5: Mechanical properties of SUPRAFORM® TM380 steel

Parameters	**Value**	**Units**
Yield Stress	380/460	MPa (min)
Tensile strength	450	MPa (min)
Elongation gauge length 50mm	(t<3.0) 20 or (t>3.0) 22	(% min)
180° Bend test (mandrel dia.)	0.5	t
Thickness (t)	2	mm

5.2.1.2. Chemical composition of the material

The relevant chemical compositions of the material are shown in Table 6.

Table 6: Chemical composition of the TM380 steel

Grade	C	Mn	Si	P (max)	S (max)	Al	Nb
TM 340	0.05	0.35	0.13	0.015	0.006	0.03	0.013
TM 380	**0.06**	**0.55**	**0.13**	**0.015**	**0.006**	**0.03**	**0.015**
TM 420	0.07	0.85	0.18	0.015	0.006	0.03	0.028
TM 460	0.08	1.15	0.18	0.015	0.006	0.03	0.033

5.2.2. SUPRAFORM® HR190

5.2.2.1. Material properties

HR190 is a much softer material compared to TM380 with improved response and ductility. This is cold rolled steel sheet primarily used for the motor vehicle industry with relevant properties as listed in Table 7.

Table 7: HR190 material parameters

Parameters	**Value**	**Units**
Yield Stress	190	MPa (min)
Tensile strength	280	MPa (min)
Elongation	36	(%)
Young's modulus	207	GPa
Poisson's ratio	0.3	-
Thickness (t)	2	mm

Typical applications of this steel are body chassis components, bumper brackets, wheel centres, and engine mounting brackets for the automotive industry.

5.2.2.2. Chemical composition of the material

The chemical composition of the material is as shown in Table 8

Table 8: Chemical composition of the HR190 steel

Grade	C	Mn	Si	Al	P	S
HR190	**0.04**	**0.20**	**0.03**	**0.04**	**0.015**	**0.015**
HR220	0.05	0.25	0.03	0.04	0.015	0.015
HR250	0.12	0.55	0.03	0.04	0.015	0.015
HR290	0.16	0.85	0.03	0.04	0.015	0.015

6. EXPERIMENTAL MEASUREMENTS

6.1. Digitising for reverse engineering using GOM System

Dimensional inspection is one of the critical steps during the manufacturing process to assure the part compliance with its design specification for controlling the quality of the product. The different variables on the production process affect geometric dimensions. One of the methods used to assess the quality of the produced part in this study involved a comparison of the pre-production part with its original CAD model.

The data for pre-production part was generated using a reverse engineering (RE) process. RE is the process of creating a 3D CAD model from an existing product. The process is performed through digitising and capturing the surface geometry of the product. In this case, the GOM scanner/GOM camera was selected due to its capacity to generate a point cloud of a surface very quickly. The accuracy of the equipment is in the tolerance band of 25-30μm, which fairly meets the general tolerances (±1 mm) of this part.

The part had to be prepared as shown in Figure 18 for digitalisation by:

- Spraying with a white powder (developed for this process) to prevent brightness from the camera-projector lamp.
- Strategically placing circular reference markers for cross reference between shots – a minimum of 3 previous markers must be seen before a new shot can be taken.

(a)

(b)

Figure 18: Physical model prepared for GOM camera

The data was generated using GOM software and refined to develop a basic setup of the 3D coordinate system. The basic 3D data was exported as STL file to further refine details such as corners, radius and holes, etc. Delcam's Powershape software was used to create surfaces on the point cloud to make a seamless model.

A satisfactory model from Powershape was imported back to GOM software to the check accuracy of RE model. The accuracy was validated by importing original CAD model (pre-production part) and superimposing over the CAD model generated through point cloud of the part to study the surface deviation

6.1.1. Results and discussion

After superimposing the RE model over original model the deviation values were noted. The superimposed model is shown in Figure 19 & 19 with a clear deviation of the surface for the object. The deviation values were found to be high near the flange radius wall where the sudden change in shape is more than 85°. The values continue to increase around the flanged wall where two angled surfaces meet. The maximum deviation observed is 0.870mm and the minimum deviation value is -0.73mm all occurred near the flanged wall. It is observed that the deviation decreases slowly in areas that are less complex in shape such flat surfaces.

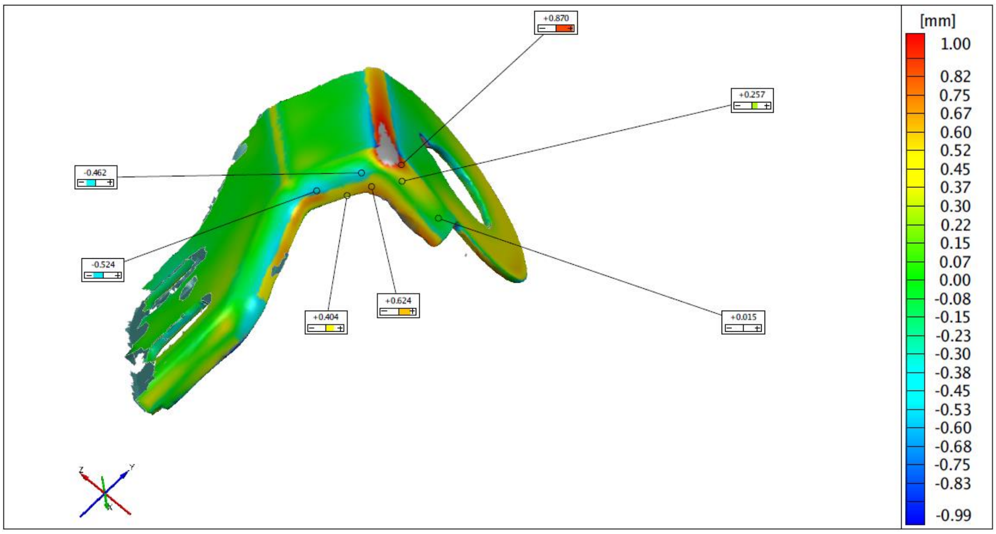

Figure 19: Snap short of superimposed model – top view

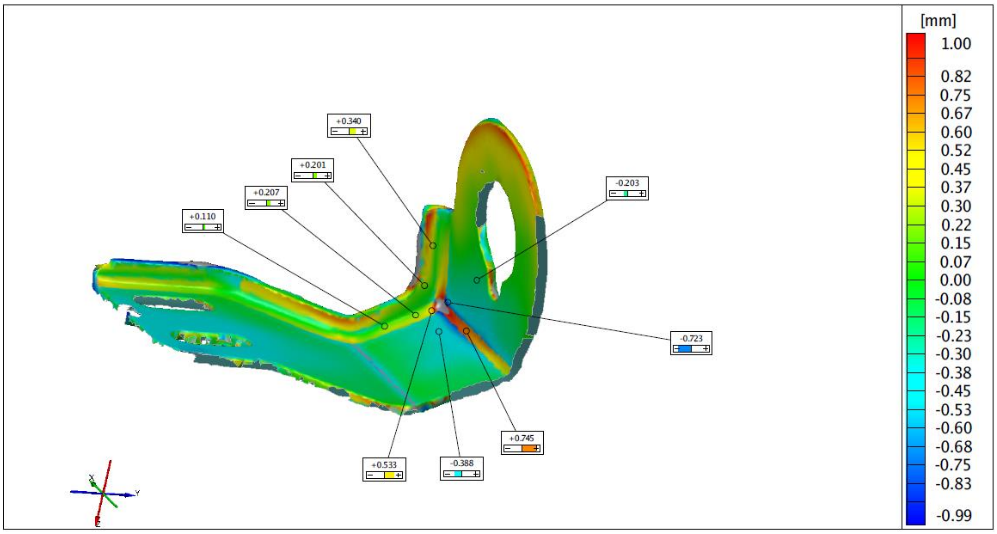

Figure 20: Snap short of superimposed model – bottom view

6.2. Measurements of deviation values of part surface at different sections using CMM

To further investigate the geometric conformity between the pre-production part and original CAD model in order to determine the measure of geometric deviation a Coordinate Measuring Machine (CMM) machine was used. The CMM machine used is a Mitutoyo Bright 710 with a calibrated accuracy of 0.001mm. The machine uses a touch probe to measure the geometry at each point.

The setup procedure of the part:

- Calibrate the touch probe on the machine table using calibration ball
- Manually select the 1 point on top of the calibration ball- the programme automatically runs and calibrates the probe
- Save the calibration settings and remove the calibration ball
- Mount the part on the CMM table using a glue gun
- Start-up the programme and select the x, y and z-direction of the part
- Save the final data and export it to excel file.

The measured surfaces are strategically divided into three zone areas. The original 3D CAD model is compared with pre-production part mounted on the CMM position. The advantage of this process is that the point measured on the part is the same point as measured on the CAD. Therefore, consistency of measurement is ensured in all directions.

6.2.1. Results and discussions

6.2.1.1. Deviation values of formed part at Zone 1 - Vertical Wall surface

Figure 21 below shows the point mapping results of the CMM quality points, with red surface denoting high and low deviations in YZ direction. The surface is twisted in Y direction with deviation values out of set acceptable forming tolerance of 0.5mm. The high and low deviation values are -0.467 to 0.366 and -0.215 to 0.917 respectively as shown in Table 9. Near the radii, the curvature is changing and the deviations found to be higher. However, the slight bend is also observed in the Z direction with deviation values within acceptable tolerance 0.130 to -0.102 and 0.06 to -0.255. It is observed that the deviation values in YZ are not following any definite pattern. The deviation values are guided by the change in curvature of the surface.

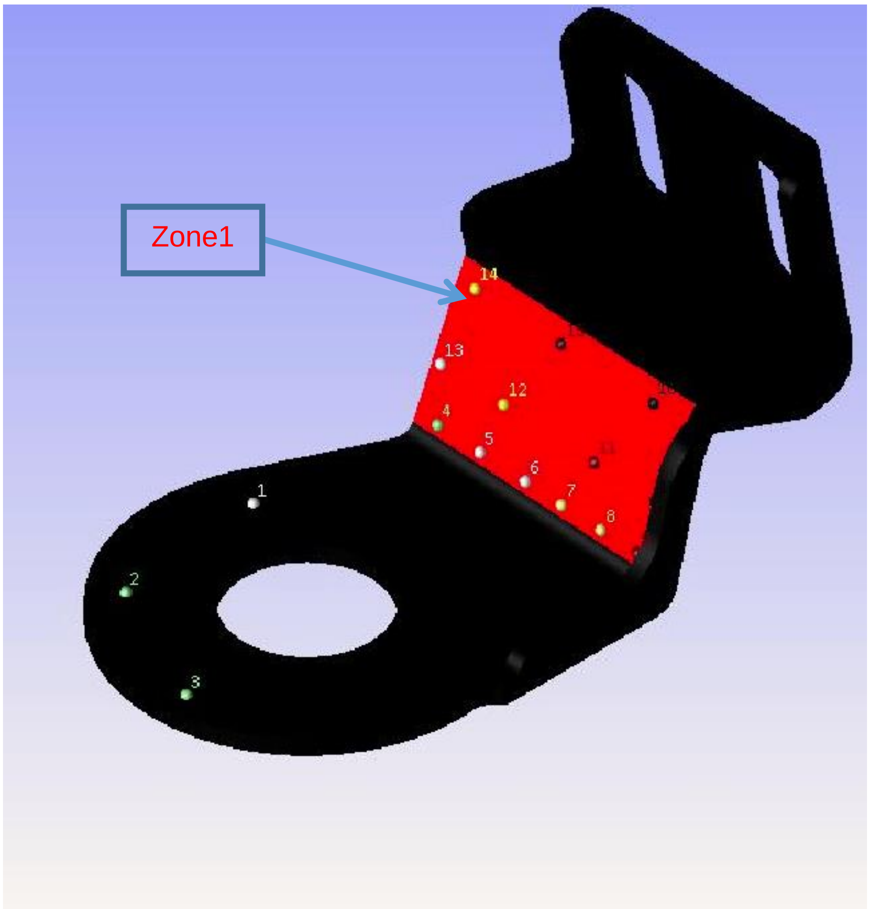

Figure 21: Vertical surface deviation in Zone1

Table 9: Deviation values of the vertical surface in Zone 1

AREA	POINTS	X	Y	Z
Zone 1	**5**	-0.012	-0.467	0.130
	12	-0.003	-0.113	0.031
	15	0.009	0.366	-0.102
	7	-0.005	-0.215	0.060
	11	0.008	0.319	-0.089
	16	0.023	0.917	-0.255

6.2.1.2. Deviation values of formed part at Zone 2 - Horizontal Flange

Figure 22 shows deviation values observed on the flanged right-angled to a flat surface. The data generated from cloud point confirms the distortion observed on the pre-production part. The deviation values observed in this zone is above the acceptable forming tolerance with a maximum deviation of 0.830 in the Z direction as seen in Table 10 point 17.

Table 10: Deviation values of the vertical surface in Zone 2

AREA	POINTS	X	Y	Z
Zone 2	**17**	-0.000	0.000	0.830
	18	0.254	-0.007	-0.394
	19	0.841	-0.022	0.235
	20	0.256	-0.007	0.000
	21	-0.021	0.025	0.044
	22	-0.106	0.003	0.008

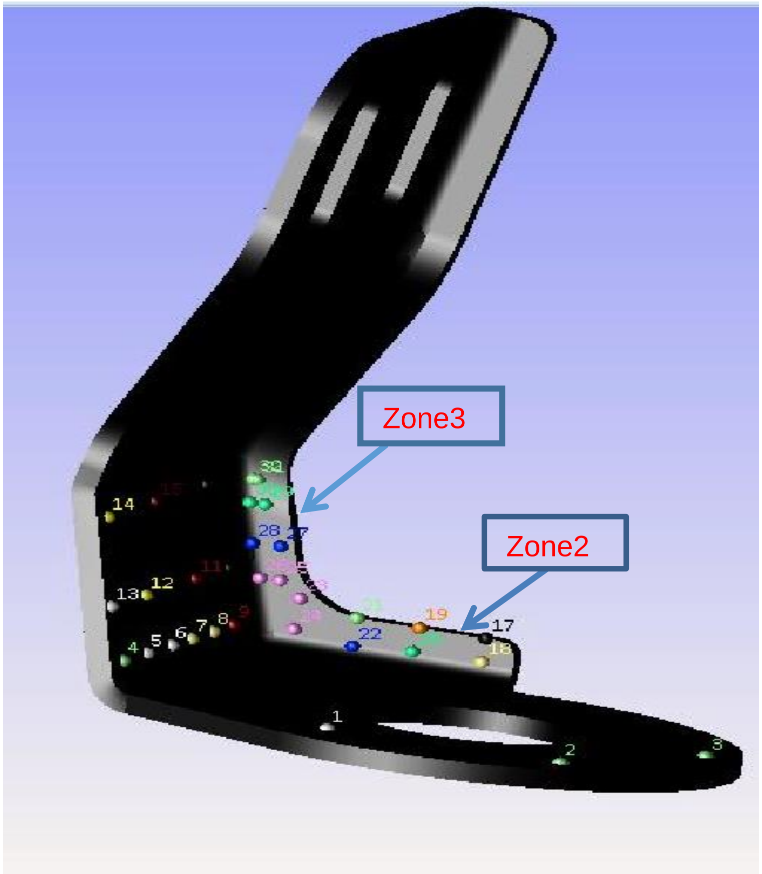

Figure 22: Horizontal flange surface in Zone2

6.2.1.3. Deviation values of formed part at Zone 3 - Vertical Flange

The flange surface depicted in Figure 22 were divided into two zones, zone 2 & 3 in order to observe the changes closely in different zones. Zone 3 is the vertical flanged surface adjacent to zone 1. The inspected point cloud showed no deviation values and they are within acceptable forming tolerance in all directions. Statistical CMM raw data is shown in **Appendix E.**

Table 11: Deviation values of the vertical surface in Zone 3

AREA	POINTS	X	Y	Z
Zone 3	**23**	-0.274	0.007	-0.000
	24	-0.245	0.006	-0.000
	25	-0.401	0.010	-0.000
	26	-0.399	-0.041	0.014
	27	-0.272	0.007	-0.000
	28	-0.367	-0.091	0.028
	29	-0.061	0.001	0.005
	30	-0.079	-0.009	0.008

7. SIMULATION RESULTS AND ANALYSIS

The multi-stage forming process was simulated at all stages with different values of coefficient of friction while keeping punch velocity constant. The optimal coefficient of friction for this setup was set 0.12 and the punch speed was kept constant at 10 m/s. The punching speed was kept constant because of the limitation on the press machine used in the press workshop. The press machine is old and punching speed cannot be changed, therefore the same punching velocity is used across all stages.

A clamping force of 200kN exerted by the blank holder for TM380 blank steel was applied to the first simulation. A number of iterations were conducted until wrinkling on the simulation model appeared reasonable.

The numerical simulation was done for the blank made of Supraform TM 380 blank steel. Therefore, the discussion of results is based on the TM380 material. This material was chosen because it is was tested experimentally in the pre-production process. The softer material, HR190 steel could not be discussed because of pending client approval for using a different material.

The results obtained by applying Ls-Dyna and Pam-Stamp have been compared to verify the manufacturing process. Comparative study of results was done on both software and results are discussed below.

7.1. Thickness variation

The thickness variation data following forming simulation results comparable to the digitalised experimental data are analysed with clear differences around points of failures. The thickness of the final part or blank sheet was 3mm with a forming tolerance of plus minus 0.5mm.

The thickness distribution of the numerical model is depicted in Figure 23 and Figure 24 with respect to different plots of Ls-Dyna and Pam-stamp software respectively. The highest values of maximum thickness are 4.34 and 3.78mm respectively. These values were observed around the compressed area of the flanged wall indicated in the figures below.

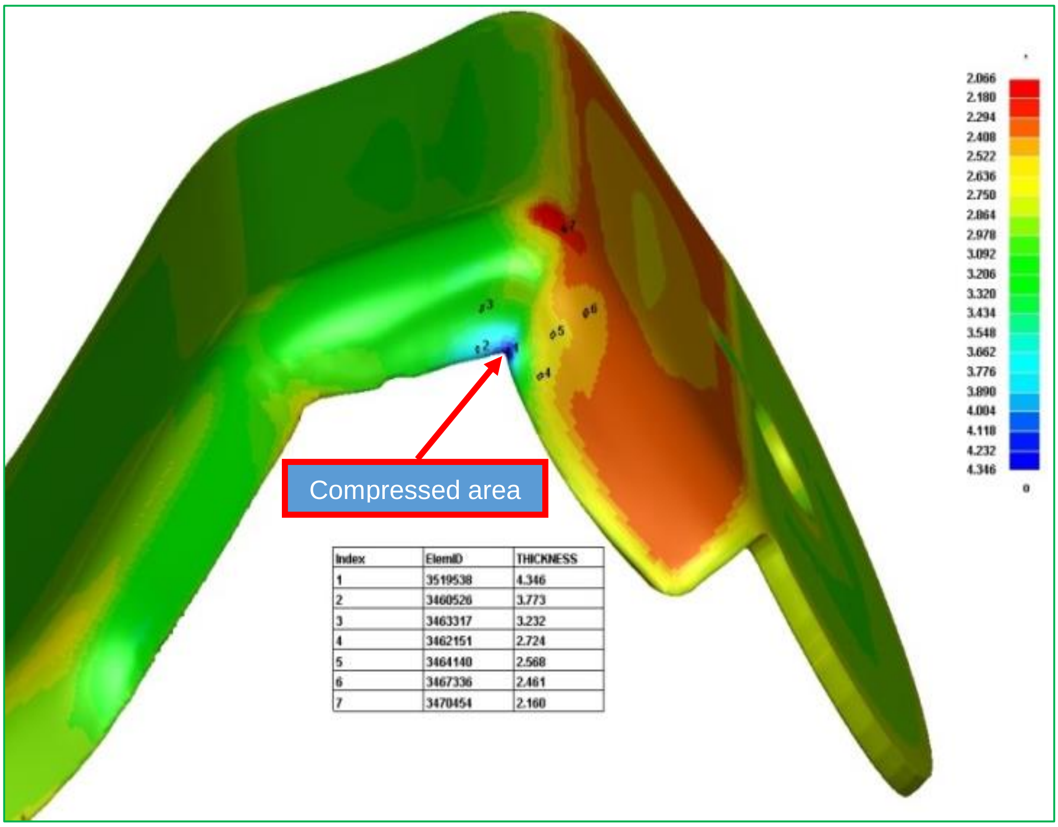

Index	ElemID	THICKNESS
1	3519538	4.346
2	3460526	3.773
3	3463317	3.232
4	3462151	2.724
5	3464140	2.568
6	3467336	2.461
7	3470454	2.160

Figure 23: Thickness variation following forming in Ls-Dyna Software

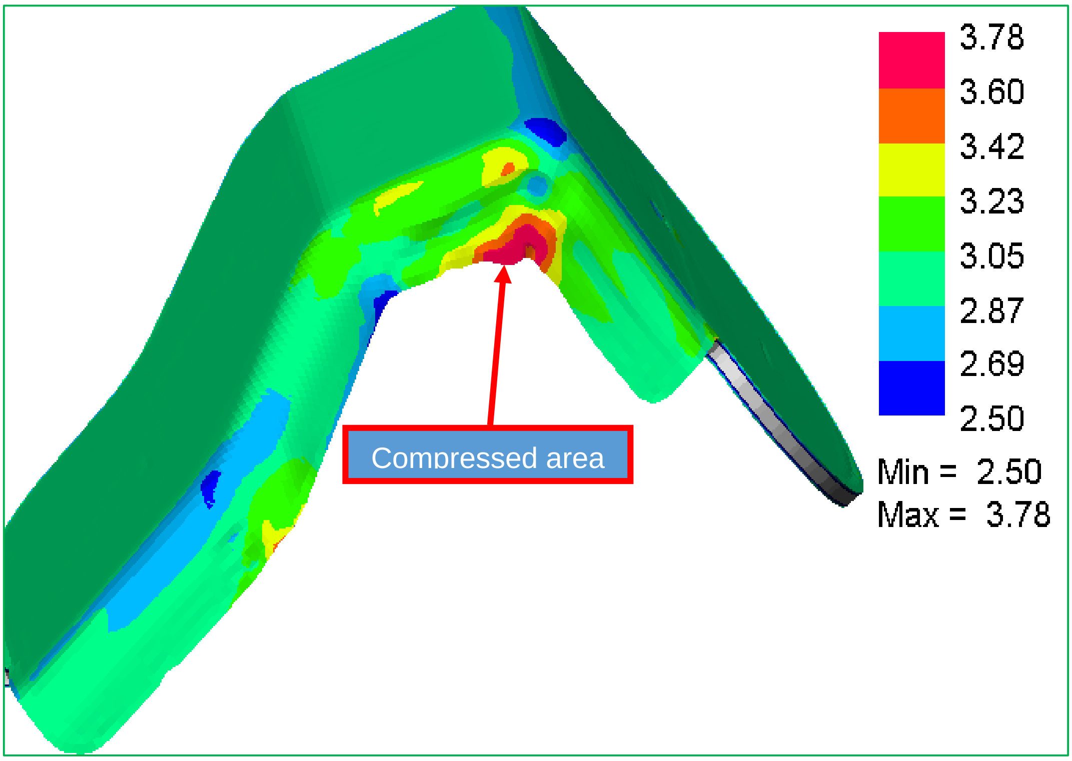

Figure 24: Thickness variation following forming in Pam-Stamp Software

The blue contours in Ls-Dyna are used to indicate the maxima, and the red contours are used to mark minima of thickness. However, in Pam-Stamp the application is quite the opposite of Ls-Dyna where the blue contours indicate minima and red contours are used to mark maxima of thickness.

Furthermore, the physical part was measured using a CMM machine for dimensional conformity. The maximum thickness value measured was 3.95mm also occurred near the flanged wall.

The comparison of the thickness variation following digitalised experimental results and numerical results of both Ls-Dyna and Pam-Stamp is presented in Table 12. The results as observed shows a correlation between the experimental and the numerical results.

The Pam-Stamp results indicate a close prediction of thickness distribution when compared with the experimental data. However, Ls-Dyna differed slightly with measured results by 0.39mm. Such agreement illustrated in the same area of the part indicates the simulation results were able to usefully predict the distortion of the part which would allow a designer to modify the tooling and processes virtually to achieve the desired outcome before going through the expense of manufacturing the tooling and setting up the production facility.

Along with this area, it can be seen that the obtained simulation results are in good agreement with pre-production results/measured results from the part.

Table 12: Thickness values from simulation at critical locations

Measured Thickening	**Simulated Thickening (Pam-Stamp)**	**Simulated Thickening (Ls-Dyna)**
3.95mm	3.78mm	4.34mm

7.2. Forming Limit Diagram (FLD) Results

Figure 25 & 26, shows the plot of the minor and major principal strain increases abruptly when the punch formed the flanged wall of the blank sheet. The flange of the blank sheet was performed on the 4th stage of the process to compensate for the vertical flange. This area marks a dramatic shape change in the blank, as the punch travels further down resulting in the formation of wrinkle with possible cracks.

The strain distribution in the flanged wall area is represented in the form of Forming Limit Curve (FLC). The possible cracks are indicated in blue on the FLC diagram and wrinkling points indicated in red. According to the results of the thickness distribution and possible failure points indicated on the FLC correspond very well with the pre-production results.

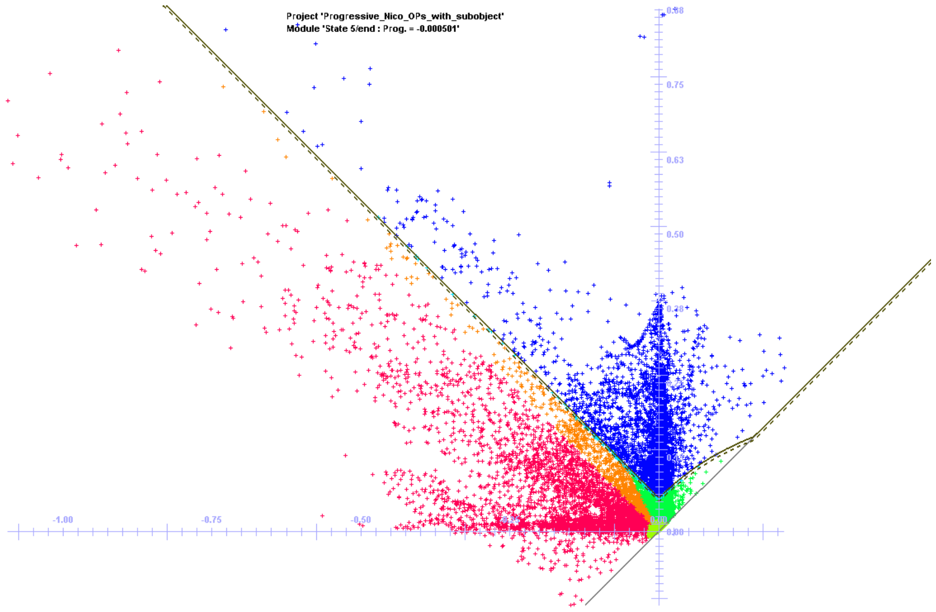

Figure 25: Representation of strain distribution using forming limit curve (FLC)

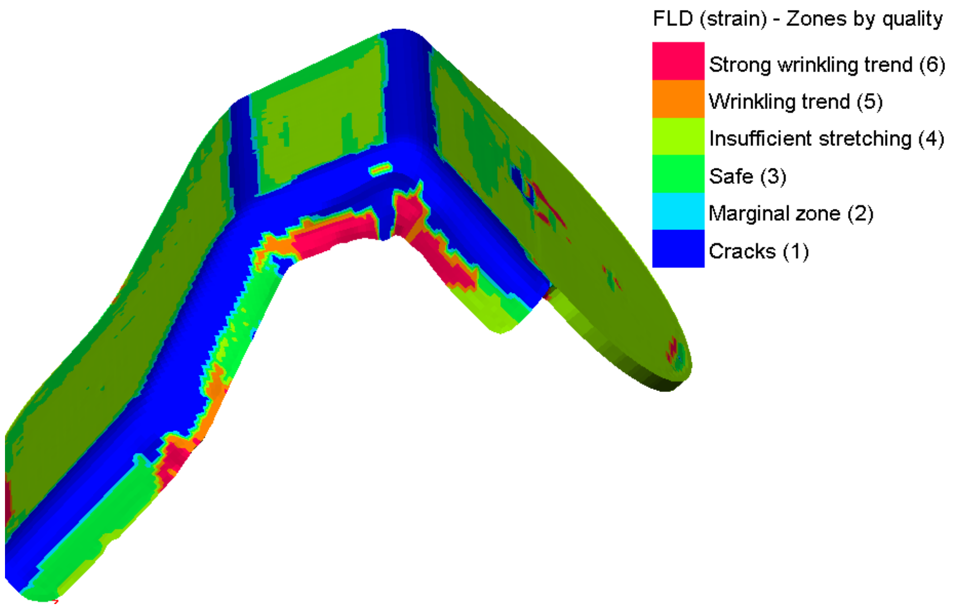

Figure 26: Representation of formability behaviour of the material

7.3. Stress distribution

The numerical results show that after the second forming stage the Von Mises stress reaches a maximum of 4.530 GPa in the area where the flange is formed on the blank sheet. See Figure 27. After the flange is formed in stage 5 the maximum Von Mises stress was reduced to 0.884 GPa as the rest of the area is at a lower stress as shown in Figure 28. The residual stress is lowered due to a redistribution of stress, which means that the patches of high stress coloured in red and yellow in the figures have been redistributed to a larger blue area. This shows that, at least from a qualitative perspective, the metal plasticity model captures the effects of the different stages of the forming process correctly. This observation suggests that the increase in a number of stages can reduce the stresses.

The highest stress concentrations are found in the areas where the forming originally developed in the forming process. The areas where the high stress prevailed after forming were those in which the angle of bend change abruptly to the region of 85º-90º had the maximum springback deformation.

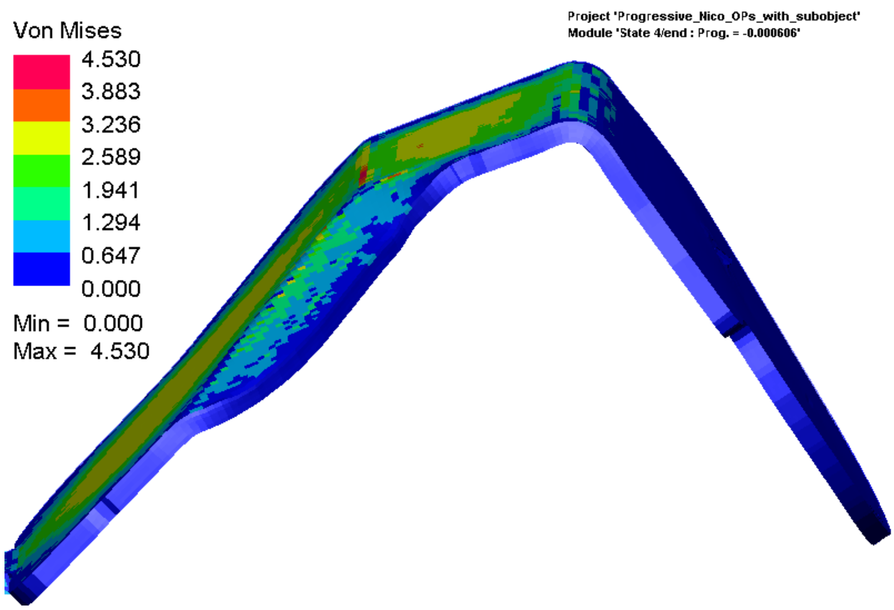

Figure 27: Pre-forming of the flange: Stage 3

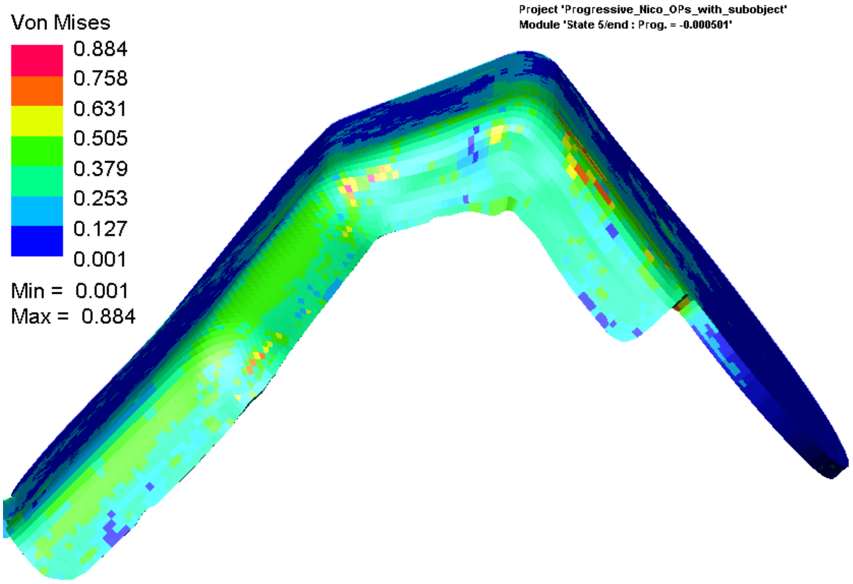

Figure 28: Final forming of the flange: Stage 5

7.4. Experimental validation of the numerical simulation against manufactured part

The numerical model was superimposed over the manufactured part. The distance between objects was calculated using the Pam-Stamp software. The numerical simulation matches the actual manufactured part as measured with CMM system. However, there was a slight deviation between the objects as seen in Figure 29. The point mapping with blue and light blue represents the final shape of the component with deviation values between 0.107 and 5.017 respectively. The deviation is highly visible on the flat surface of the model far from the critical radius of 3mm. This deviation could be attributed to springback behaviour. The springback was found to be in the region of 0.4 -1.09mm. This exceeds the acceptable allowable tolerance with respect to the final desired part of 0±0.9mm.

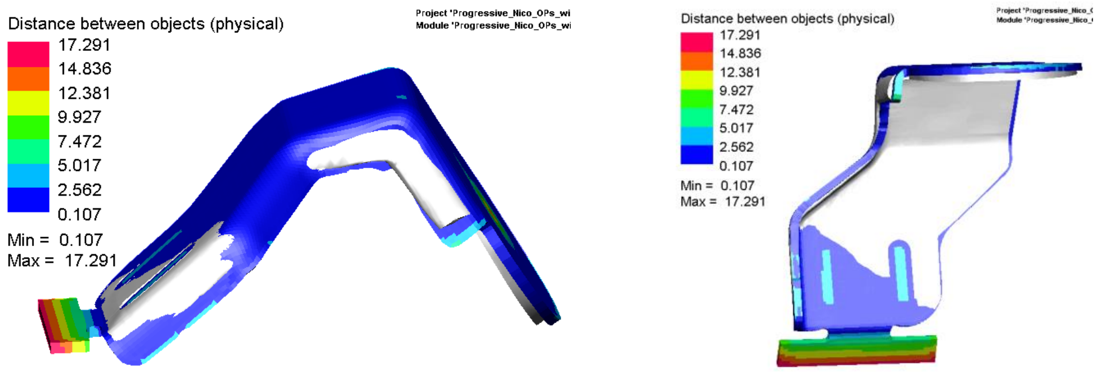

Figure 29: The distance between numerical model and manufactured part

8. CONCLUSION

The discussion above illustrated a successful numerical simulation of a 5-stage forming process of Supraform TM 380 blank materials using Ls-Dyna and Pam-Stamp software packages. A number of material and process parameters had to be input into the explicit dynamic finite element analysis with contact and friction which makes this analysis more complex than for example static structural analyses.

The numerical result as shown in Figure 27 shows that after the flanging stage the Von Mises stress reaches a maximum 4.530 GPa in the area near the angled surface walls of the last bend from the formed blank where the greatest thickening occurs.

With reference to the flange area, the maximum thickening of the measured part is found to be 3.95mm and the simulated one for Pam-Stamp and Ls-Dyna are found to be 3.78mm and 4.34mm respectively. The measured thickening of 3.95mm exceeded the maximum acceptable increase in material thickness. The acceptable increase in material thickness due to forming should not be greater than 10% of the blank thickness.

Cracking trend near the 3mm radius is also a potential problem indicated by the simulation. The tensile stress needs to be reduced in this area. This could be achieved by changing the die geometry and/or loads and forming speeds used. An alternative solution would be to add a metal gainer but this would add another step in the forming process.

The highest stress concentrations are found in the areas where the forming originally developed in the forming process. The areas where the high stress prevailed after forming were those in which the angle of bend changes abruptly in the region of 85º-90º

The results produced shows that the simulation process accurately predicted the final shape of the part with noted failures. Therefore, the simulation method can be repeated for different tooling and process parameters to arrive at an acceptable finished part without having to physically manufacture the tooling and set up the plant.

Future work in relation to this optimisation framework includes the attempt to reduce the number of forming stages and investigation of the dimensional conformance of the part for different material choices.

9. REFERENCES

Aghaie-khafri, M., Mahmudi, R. & Pishbin, H., 2002. Role of Yield Criteria and Hardening Laws in the Prediction of Forming Limit Diagrams. *Metallurgical and Materials Transactions,* Issue 33, pp. 1363-1371.

Altan, T. & Vasquez, T., 2000. New Concepts in Die Design- Physical and Computer Modelling. *Journal of Materials Processing Technology,* Issue 98, pp. 212-223.

Bai, Y. & Wierzbicki, T., 2007. A New Model of Metal Plasticity and Fracture with Pressure and Lode Dependence. *International Journal of Plasticity,* pp. 1072-1073.

De-hua, H., Xiao-qiang, L., Dong-sheng, L. & Wei-jun, Y., 2010. Process Design for Multi-stage Stretch Forming of Aluminium Alloy Aircraft Skin. *Transactions of Nonferrous Metals Society of China,* 20(6), pp. 1053-1058.

Dixit, U., Josh, S. & Davim, J., 2011. Incorporation of Material Behavior in Modeling of Metal Forming and Machining Processes. *Materials and Designs,* Volume 32, pp. 3655-3670.

Dynamore Support, 2015. *Calculation of Hill Parameters from Given r-values for Solid Elements,* Stuttgart: s.n.

Eliseev, V. V., 1991. Calculation of transition in strecht forming. *Soviet Aeronautics,* Volume 34(2), pp. 108-111.

ETA/DYNAFORM, 2006. *ETA/DYNAFORM User's Manual.* 5.5 ed. Troy, MI: Engineering Technology Associations Inc.

ETA/DYNAFORM, 2006. *User's Manual Version 5.5,* MI, USA: Engineering Technology Associations Inc.

Fang, Y. et al., 2014. Analytical and Experimental Investigations on Deformation Mechanism and Fracture Behaviour in Single Point Incremental Forming. *Materials Processing Technology,* Issue 214, pp. 1503-1515.

Finn, M., Gallbraith, P., Wu, L. & Hallquist, J., 1995. Use of a Coupled Solver for Calculation Spring-back in Automotive Body Panels. *Journal of Materials Processing Technology,* pp. 395-409.

Gang, F., Qing-jun, L., Li-ping, L. & Pan, Z., 2012. Comperative Analysis Between Stress-and Strain-based Forming Limit Diagrams for Aluminum Alloy Sheet 1060. *Transactions of Nonferrous Metals Society of China,* Volume 22, pp. 343-349.

Goel, A., 2004. *Blank Optimisation in Sheet Metal Forming using Finite Element Simulation,* Chicago: Texas A & M University.

Hallquist, J., 2007. *Ls-Dyna Keyword User's Manual.,* Livermore CA: Livermore Software Corparation.

He, J. et al., 2013. Sheet Metal Forming Limits Under Stretch-bending with Anisotropic Hardening. *International journal of mechanical science,* Issue 75, pp. 244-256.

Janbakhsh, M., Loghmanian, S. & Djavanroodi, F., 2014. Application of Different Hill's Yield Criteria to Predict Limit Strains for Aerospace Titanium and Aluminum Sheet Alloys. *Advanced Design and Manufacturing Technology,* 7(1), pp. 36-38.

Jan, S. & Miroslav, J., 2012. Springbaack Prediction in Sheet Metal Forming Processes. *Journal for Technology of Plasticity,* 37(1), p. 94.

Jayahari, L. et al., 2012. Formability Studies of ASS 304 and Evaluation of Friction for Al in Deep Drawing Setup at Elevated Temperatures Using LS-DYNA. *Journal of King Saud University,* Volume 26, pp. 21-31.

Kotkunde, N., Deole, A., Gupta, A. & Singh, S., 2014. Experimental and Numerical Investigation of Anisotropic Yield Criteria for Warm Deep Drawing of Ti–6Al–4V Alloy. *Materials and Design,* Issue 63, pp. 336-344.

Kurra, S. & Srinivasa, P. R., 2014. Analysis of Formability in Single Point Incremental Forming Using Finite Element Simulation. *Procedia Material Science,* pp. 430-435.

Ls-Dyna, 2007. *Ls-Dyna Support.* [Online] Available at: http://www.dynasupport.com/tutorial/ls-dyna-users-guide/contact-modeling-in-ls-dyna [Accessed 16 11 2015].

Ls-Dyna, 2012. *Keyword User's Manual ,* Livermore: LIVERMORE SOFTWARE TECHNOLOGY CORPORATION .

Morris, A., 2008. *A practical guide to reliable finite element modelling..* s.l.:John Wiley and Sons.

Nagpal, G., 2004. *Tool Engineering and Design.* 6 ed. Delhi: Khanna.

PAM-STAMP, 2015. *PAM-STAMP 2015.1 User's Guide.* s.l.:ESI Group.

Park, D., Huh, H. & Kim, S., 2004. A Four-node Shell Element with Enhanced Bending Perfomence for Springback Analysis. *Computer Methods in Applied mechanics and Engineering,* 193(23-26), pp. 2105-2138.

Schimid, 2008. *Sheet-Metal Forming Process,* s.l.: Pearson Education.

Shi, M., Zhu, X., Xia, Z. & Stoughton, T., 2008. Determination of nonlinear isotropic/kinematic hardening constitutive paramaters for AHSS using tension and compression tests. *Numisheet,* pp. 137-148.

Song, J., Huh, H. & Kim, S., 2007. A Simulation Based Parameter Studying the Stamping Process of an Automotive Member. *Journal of Material Processing Technology,* Issue 189, pp. 450-458.

Statssa, 2012. *Statistics South Africa.* [Online] Available at: http://www.statssa.gov.za/publications/SAStatistics/SAStatistics2012.pdf [Accessed 16 09 2015].

Teherizadeh, A., Green, D. & Yoon, J., 2015. A Non-associated Plasticity Model with Anisotropic and Nolinear Kinematic Harderning for Simulation of Sheet Metal Forming. *International Journal of Solids and Structures,* pp. 371-372.

Tisza, M., 2004. Numerical modelling and simulation in sheet metal forming. *Material Processing Technology,* 151(1-3).

Tisza, M., Likacs, Z. & G., G., 2008. Integrated Process Simulation and Die-Design in Sheet Metal Forming. *International Journal of Material Forming,* pp. 185-188.

Wang, E., 2006. *Thin-wall Structures Simulation.* Germany, s.n.

YU, Z., 2006. Study On Numerical Simulation Of Multi-stage Deep Drawing Process Of Sheet Metal. *Materials science,* Issue 2121360155972644.

10. APPENDICES

Appendix A: Definition of material or the HR190 using values of Lankford and Hill’s parameters

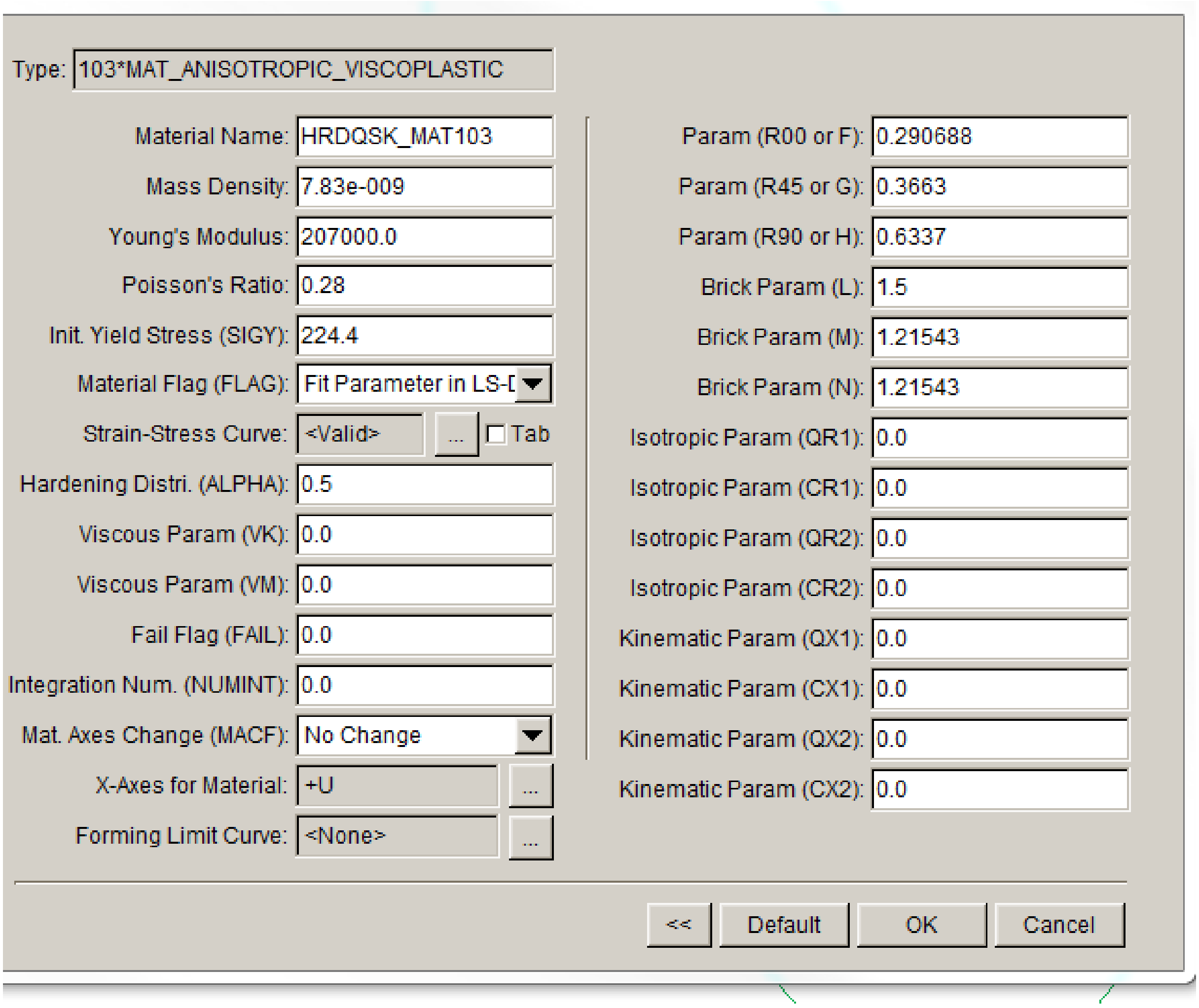

Appendix B: Definition of material or the TM380 using values of Lankford and Hill's parameters

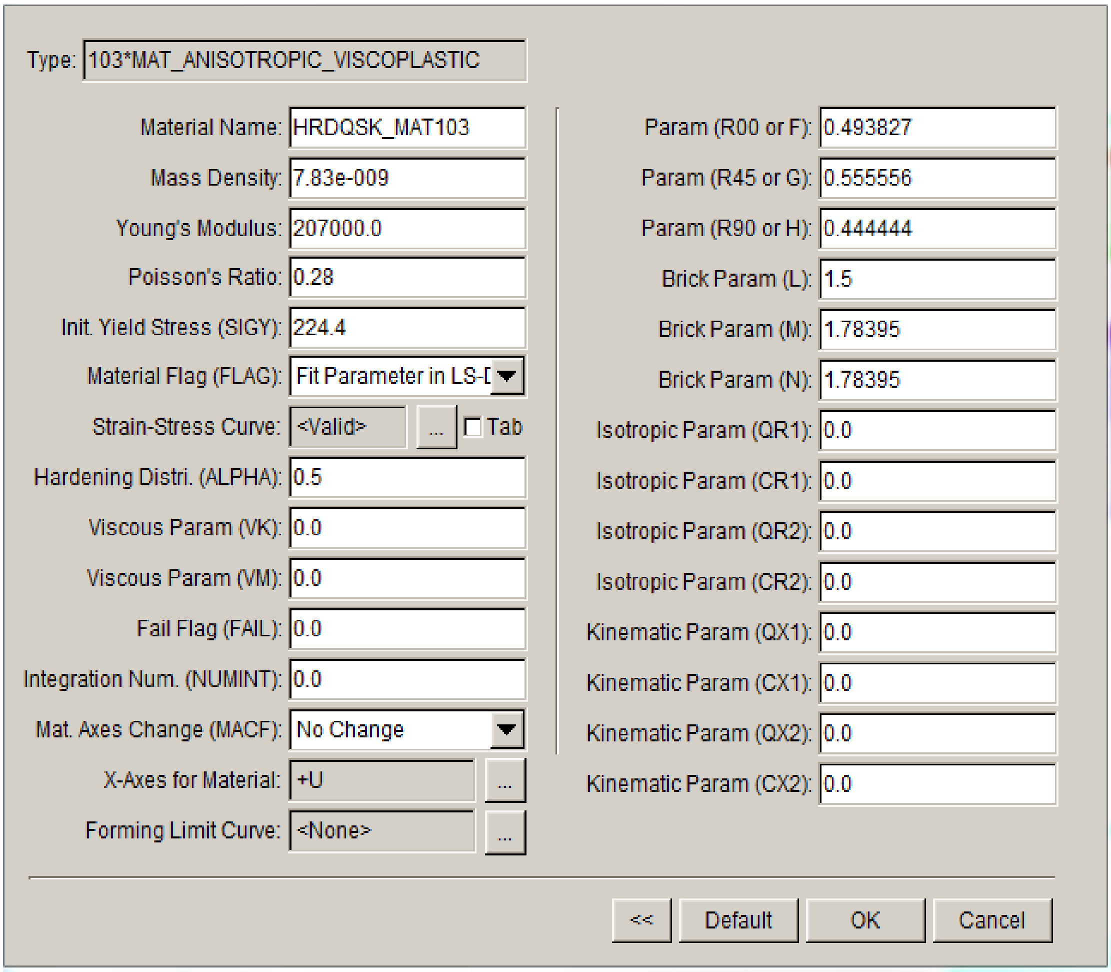

Appendix C: Input deck continuum model for TM380

```
$ ETA/DYNAFORM : LS-DYNA(971R5+) INPUT DECK
$ DATE : Nov 04, 2015 at 10:57:54
$ VERSION : eta/DYNAFORM 5.9.2, built on Sep  4 2014
$ EXPORTER : AUTO-SETUP
$
$ VIEWING INFORMATION
$  -882.572753 -274.756561 -253.398834 87.27664948
$         1.0         0.0         0.0
$         0.0         1.0         0.0
$         0.0         0.0         1.0
$
$ UNIT SYSTEM: MM, TON, SEC, N
$
$ SIMULATION  : SHEET FORMING
$ RCMD-SOLVER : SINGLE
$
$---+----1----+----2----+----3----+----4----+----5----+----6----+----7----+----8
$
*KEYWORD_JOBID
Simulation_2_mod_op60
$
$---+----1----+----2----+----3----+----4----+----5----+----6----+----7----+----8
$
$                (1) TITLE CARD
$
$---+----1----+----2----+----3----+----4----+----5----+----6----+----7----+----8
*TITLE
forming / untitled
$---+----1----+----2----+----3----+----4----+----5----+----6----+----7----+----8
$
$                (2) DEFINE PARAMETERS
$
$---+----1----+----2----+----3----+----4----+----5----+----6----+----7----+----8
*PARAMETER
$    PRMR1      VAL1     PRMR2      VAL2     PRMR3      VAL3     PRMR4      VAL4
  R SCALEF       1.0
$---+----1----+----2----+----3----+----4----+----5----+----6----+----7----+----8
```

```
$
$                 (3) CONTROL CARDS
$
$---+----1----+----2----+----3----+----4----+----5----+----6----+----7----+----8
*CONTROL_TERMINATION
$   ENDTIM    ENDCYC     DTMIN    ENDNEG    ENDMAS
0.06754518         0                     0.0
*CONTROL_TIMESTEP
$   DTINIT    TSSFAC      ISDO    TSLIMT     DT2MS      LCTM     ERODE     MS1ST
       0.0       0.9         0       0.0 -3.85E-07
$   DT2MSF   DT2MSLC     IMSCL
                             0
*CONTROL_RIGID
$      LMF      JNTF    ORTHMD     PARTM    SPARSE    METALF
                                                          1
*CONTROL_HOURGLASS
$      IHQ        QH
         5       0.1
*CONTROL_BULK_VISCOSITY
$       Q1        Q2      TYPE
       1.5      0.06        -2
*CONTROL_SHELL
$   WRPANG     ESORT     IRNXX    ISTUPD    THEORY       BWC     MITER      PROJ
      20.0         1        -1         1         2         2         1         0
$  ROTASCL    INTGRD    LAMSHT    CSTYP6    TSHELL    NFAIL1    NFAIL4

$  PSSTUPD    IRQUAD

$   NFAIL1    NFAIL4   PSNFAIL    KEEPCS     DELFR
         1         1
*CONTROL_SOLID
$    ESORT    FMATRX   NIPTETS    SWLOCL
         1         0         4         2
*CONTROL_CONTACT
$   SLSFAC    RWPNAL    ISLCHK    SHLTHK    PENOPT    THKCHG     ORIEN
      0.08       0.0         2         1         4         0         1
$   USRSTR    USRFAC     NSBCS    INTERM     XPENE     SSTHK      ECDT   TIEDPRJ
```

```
        0         0       10         0       1.0         0
*CONTROL_ENERGY
$     HGEN      RWEN    SLNTEN     RYLEN
        2         1         2         1
*CONTROL_OUTPUT
$    NPOPT    NEECHO    NREFUP    IACCOP     OPIFS    IPNINT    IKEDIT
        1         0         0         0       0.0         0       100
*CONTROL_PARALLEL
$     NCPU    NUMRHS     CONST
        1         0         2
*CONTROL_ACCURACY
$      OSU       INN
        0         1
*INTERFACE_SPRINGBACK_LSDYNA
$     PSID      NSHV
        1       100
*CONTROL_MPP_IO_NODUMP
$---+----1----+----2----+----3----+----4----+----5----+----6----+----7----+----8
$*DATABASE_OPTION
$       DT    BINARY
$OPTION : SECFORC RWFORC NODOUT ELOUT  GLSTAT
$         DEFORC  MATSUM NCFORC RCFORC DEFGEO
$         SPCFORC SWFORC ABSTAT NODFOR BNDOUT
$         RBDOUT  GCEOUT SLEOUT MPGS   SBTOUT
$         JNTFORC AVSFLT MOVIE
*DATABASE_RCFORC
6.7545E-05
*DATABASE_MATSUM
6.7545E-05
*DATABASE_GLSTAT
6.7545E-05
*DATABASE_SLEOUT
6.7545E-05
*DATABASE_RBDOUT
6.7545E-05
*DATABASE_BNDOUT
6.7545E-05
```

```
*DATABASE_ABSTAT
6.7545E-05
$---+----1----+----2----+----3----+----4----+----5----+----6----+----7----+----8
*DATABASE_BINARY_D3PLOT
$  DT/CYCL     LCDT     BEAM
             21
*DATABASE_EXTENT_BINARY
$   NEIPH    NEIPS   MAXINT   STRFLG   SIGFLG   EPSFLG   RLTFLG   ENGFLG
        0        0        7        1
$   CMPFLG   IEVERP   BEAMIP    DCOMP     SHGE    STSSZ
              1                 2
$---+----1----+----2----+----3----+----4----+----5----+----6----+----7----+----8
$
$                 (4) DEFINE BLANK
$
$---+----1----+----2----+----3----+----4----+----5----+----6----+----7----+----8
*SET_PART_LIST
$SET_PART_NAME: BLANK
$     SID      DA1      DA2      DA3      DA4
        1
$    PID1     PID2     PID3     PID4     PID5     PID6     PID7     PID8
      122
*PART
$HEADING
 PART PID =      122 PART NAME :NEW_BLK
$     PID    SECID      MID    EOSID     HGID     GRAV   ADPOPT     TMID
      122       15       15
*MAT_ANISOTROPIC_VISCOPLASTIC
$MATERIAL NAME:HRDQSK_MAT103
$     MID       RO        E       PR     SIGY     FLAG     LCSS    ALPHA
       15  7.83E-09  2.07E+05     0.28     224.4      1.0       22      0.5
$     QR1      CR1      QR2      CR2      QX1      CX1      QX2      CX2

$      VK       VM  R00 or F  R45 or G  R90 or H        L        M        N
      0.0      0.0  0.493827  0.555556  0.444444      1.5   1.78395   1.78395
$    AOPT     FAIL   NUMINT     MACF
      2.0      0.0      0.0        1
```

```
$       XP        YP        ZP        A1        A2        A3
                              1.0       0.0       0.0
$       V1        V2        V3        D1        D2        D3      BETA
                              0.0       1.0       0.0
*SECTION_SOLID
$    SECID    ELFORM       AET
        15         1
$---+----1----+----2----+----3----+----4----+----5----+----6----+----7----+----8
$
$                   (5) DEFINE TOOLS
$
$---+----1----+----2----+----3----+----4----+----5----+----6----+----7----+----8
$---+----1----+----2----+----3----+----4----+----5----+----6----+----7----+----8
$                   TOOL < 60_die >
$---+----1----+----2----+----3----+----4----+----5----+----6----+----7----+----8
*SET_PART_LIST
$SET_PART_NAME: 60_die
$      SID       DA1       DA2       DA3       DA4
        14
$     PID1      PID2      PID3      PID4      PID5      PID6      PID7      PID8
        88
*PART
$HEADING
 PART PID =       88 PART NAME :DIE00004
$      PID     SECID       MID     EOSID      HGID      GRAV    ADPOPT      TMID
        88        16        16
*MAT_RIGID
$      MID        RO         E        PR         N    COUPLE         M     ALIAS
        16  7.83E-09  2.07E+05      0.28
$      CMO      CON1      CON2
         1         7         7
$LCO or A1        A2        A3        V1        V2        V3

*SECTION_SHELL
$    SECID    ELFORM      SHRF       NIP     PROPT   QR/IRID     ICOMP     SETYP
        16         2       1.0       3.0       0.0
$       T1        T2        T3        T4      NLOC
```

```
       1.0       1.0       1.0       1.0
*CONTACT_FORMING_ONE_WAY_SURFACE_TO_SURFACE_ID
$      CID  CONTACT INTERFACE TITLE
        11  BLANK/60_die
$     SSID      MSID     SSTYP     MSTYP    SBOXID    MBOXID       SPR       MPR
         1        14         2         2                             1         1
$       FS        FD        DC        VC       VDC    PENCHK        BT        DT
     0.125       0.0       0.0       0.0      20.0         0       0.0     1E+20
$      SFS       SFM       SST       MST      SFST      SFMT       FSF       VSF
       0.0       0.0       0.0       0.0
$     SOFT   SOFSCL    LCIDAB    MAXPAR    PENTOL     DEPTH     BSORT    FRCFRQ
         0
$   PENMAX    THKOPT    SHLTHK     SNLOG      ISYM     I2D3D    SLDTHK    SLDSTF
                             1
$     IGAP    IGNORE    DPRFAC    DTSTIF                        FLANGL
         1
$---+----1----+----2----+----3----+----4----+----5----+----6----+----7----+----8
$                 TOOL < 60_punch >
$---+----1----+----2----+----3----+----4----+----5----+----6----+----7----+----8
*SET_PART_LIST
$SET_PART_NAME: 60_punch
$      SID       DA1       DA2       DA3       DA4
        15
$     PID1      PID2      PID3      PID4      PID5      PID6      PID7      PID8
        90
*PART
$HEADING
 PART PID =        90 PART NAME :PUNCH004
$      PID     SECID       MID     EOSID      HGID      GRAV    ADPOPT      TMID
        90        17        17
*MAT_RIGID
$      MID        RO         E        PR         N    COUPLE         M     ALIAS
        17  7.83E-09  2.07E+05      0.28
$      CMO      CON1      CON2
         1         4         7
$LCO or A1        A2        A3        V1        V2        V3
```

```
*SECTION_SHELL
$   SECID   ELFORM     SHRF      NIP    PROPT  QR/IRID    ICOMP    SETYP
       17        2      1.0      3.0      0.0
$      T1       T2       T3       T4     NLOC
      1.0      1.0      1.0      1.0
*CONTACT_FORMING_ONE_WAY_SURFACE_TO_SURFACE_ID
$     CID  CONTACT INTERFACE TITLE
       12  BLANK/60_punch
$    SSID     MSID    SSTYP    MSTYP   SBOXID   MBOXID      SPR      MPR
        1       15        2        2                          1        1
$      FS       FD       DC       VC      VDC   PENCHK       BT       DT
    0.125      0.0      0.0      0.0     20.0        0      0.0    1E+20
$     SFS      SFM      SST      MST     SFST     SFMT      FSF      VSF
      0.0      0.0      0.0      0.0
$   SOFT   SOFSCL   LCIDAB   MAXPAR   PENTOL    DEPTH    BSORT   FRCFRQ
        0
$  PENMAX   THKOPT   SHLTHK    SNLOG     ISYM    I2D3D   SLDTHK   SLDSTF
                              1
$    IGAP   IGNORE   DPRFAC   DTSTIF                     FLANGL
        1
$---+----1----+----2----+----3----+----4----+----5----+----6----+----7----+----8
$                 TOOL < 60_binder >
$---+----1----+----2----+----3----+----4----+----5----+----6----+----7----+----8
*SET_PART_LIST
$SET_PART_NAME: 60_binder
$     SID      DA1      DA2      DA3      DA4
       16
$    PID1     PID2     PID3     PID4     PID5     PID6     PID7     PID8
      102
*PART
$HEADING
 PART PID =      102 PART NAME :GENSRF0
$     PID    SECID      MID    EOSID     HGID     GRAV   ADPOPT     TMID
      102       18       18
*MAT_RIGID
$     MID       RO        E       PR        N   COUPLE        M    ALIAS
       18  7.83E-09  2.07E+05     0.28
```

```
$     CMO     CON1     CON2
       1        4        7
$LCO or A1       A2       A3       V1       V2       V3

*SECTION_SHELL
$    SECID    ELFORM     SHRF      NIP     PROPT   QR/IRID     ICOMP     SETYP
      18         2      1.0      3.0      0.0
$      T1       T2       T3       T4     NLOC
      1.0      1.0      1.0      1.0
*CONTACT_FORMING_ONE_WAY_SURFACE_TO_SURFACE_ID
$      CID  CONTACT INTERFACE TITLE
      13  BLANK/60_binder
$     SSID     MSID     SSTYP     MSTYP    SBOXID    MBOXID      SPR      MPR
       1       16        2        2                       1        1
$       FS       FD       DC       VC      VDC    PENCHK       BT       DT
    0.125      0.0      0.0      0.0     20.0        0      0.0    1E+20
$      SFS      SFM      SST      MST     SFST     SFMT      FSF      VSF
      0.0      0.0      0.0      0.0
$     SOFT   SOFSCL   LCIDAB   MAXPAR   PENTOL    DEPTH    BSORT   FRCFRQ
       0
$  PENMAX   THKOPT   SHLTHK    SNLOG     ISYM    I2D3D   SLDTHK   SLDSTF
                           1
$     IGAP   IGNORE   DPRFAC   DTSTIF                    FLANGL
       1
$---+----1----+----2----+----3----+----4----+----5----+----6----+----7----+----8
$
$                 (6) DEFINE PROCESS STEPS
$
$---+----1----+----2----+----3----+----4----+----5----+----6----+----7----+----8
$---+----1----+----2----+----3----+----4----+----5----+----6----+----7----+----8
$                 STEP < closing >
$---+----1----+----2----+----3----+----4----+----5----+----6----+----7----+----8
$60_die : stationary
$60_punch : stationary
*BOUNDARY_PRESCRIBED_MOTION_RIGID
$   typeID      DOF      VAD     LCID       SF      VID    DEATH    BIRTH
      90        3        0       23     -1.0       00.02892682      0.0
```

```
$60_binder : velocity
*BOUNDARY_PRESCRIBED_MOTION_RIGID
$   typeID      DOF      VAD      LCID       SF      VID     DEATH     BIRTH
      102        3        0       24      -1.0        00.02892682       0.0
$---+----1----+----2----+----3----+----4----+----5----+----6----+----7----+----8
$                   STEP < drawing >
$---+----1----+----2----+----3----+----4----+----5----+----6----+----7----+----8
$60_die : stationary
$60_punch : velocity
*BOUNDARY_PRESCRIBED_MOTION_RIGID
$   typeID      DOF      VAD      LCID       SF      VID     DEATH     BIRTH
       90        3        0       25      -1.0        00.067545180.02892682
$60_binder : force
*LOAD_RIGID_BODY
$      PID      DOF      LCID       SF      CID       M1       M2       M3
      102        3       26      -1.0        0
*CONSTRAINED_RIGID_BODY_STOPPERS
$      PID    LCMAX     LCMIN    PSIDMX    PSIDMN    LCVMNX      DIR      VID
      102      -27         0         0         0         0        4        3
$       TB       TD
0.028926820.06854518
$---+----1----+----2----+----3----+----4----+----5----+----6----+----7----+----8
$
$                   (7) DEFINE CURVES
$
$---+----1----+----2----+----3----+----4----+----5----+----6----+----7----+----8
*DEFINE_CURVE
$D3PLOT
$     LCID     SIDR     SCLA     SCLO     OFFA     OFFO    DATTYP
       21        0
$               A1                  O1
   0.0000000000E+00    5.7853651538E-03
   5.7853651538E-03    5.7853651538E-03
   1.1570730308E-02    5.7853651538E-03
   1.7356095461E-02    5.7853651538E-03
   2.3141460615E-02    5.7853651538E-03
   2.8926825769E-02    5.5040435791E-04
```

```
   2.9477230127E-02    1.0067985091E-02
   3.9545215218E-02    4.9999910240E-03
   4.4545206243E-02    4.9999910240E-03
   4.9545197267E-02    4.9999910240E-03
   5.4545188291E-02    2.4999955120E-03
   5.7045183803E-02    2.4999955120E-03
   5.9545179315E-02    2.4999955120E-03
   6.2045174827E-02    2.4999955120E-03
   6.4545170339E-02    1.0000261424E-03
   6.5545196481E-02    9.9999122041E-04
   6.6545187701E-02    1.0000000000E-03
   6.7545187701E-02    1.0000000000E-03
*DEFINE_CURVE
$SSC
$     LCID      SIDR      SCLA      SCLO      OFFA      OFFO    DATTYP
        22         0
$                 A1                  O1
   0.0000000000E+00    2.2098000000E+02
   2.0000000000E-03    2.2838000000E+02
   4.0000000000E-03    2.3499000000E+02
   6.0000000000E-03    2.4099000000E+02
   8.0000000000E-03    2.4649000000E+02
   1.0000000000E-02    2.5157000000E+02
   1.2000000000E-02    2.5630000000E+02
   1.4000000000E-02    2.6074000000E+02
   1.6000000000E-02    2.6491000000E+02
   1.8000000000E-02    2.6886000000E+02
   2.0000000000E-02    2.7261000000E+02
   2.2000000000E-02    2.7618000000E+02
   2.4000000000E-02    2.7958000000E+02
   2.6000000000E-02    2.8284000000E+02
   2.8000000000E-02    2.8597000000E+02
   3.0000000000E-02    2.8898000000E+02
   3.2000000000E-02    2.9188000000E+02
   3.4000000000E-02    2.9468000000E+02
   3.6000000000E-02    2.9738000000E+02
   3.8000000000E-02    3.0000000000E+02
```

4.0000000000E-02	3.0254000000E+02
4.2000000000E-02	3.0500000000E+02
4.4000000000E-02	3.0739000000E+02
4.6000000000E-02	3.0971000000E+02
4.8000000000E-02	3.1198000000E+02
5.0000000000E-02	3.1418000000E+02
5.2000000000E-02	3.1633000000E+02
5.4000000000E-02	3.1843000000E+02
5.6000000000E-02	3.2047000000E+02
5.8000000000E-02	3.2248000000E+02
6.0000000000E-02	3.2443000000E+02
6.2000000000E-02	3.2635000000E+02
6.4000000000E-02	3.2822000000E+02
6.6000000000E-02	3.3006000000E+02
6.8000000000E-02	3.3186000000E+02
7.0000000000E-02	3.3362000000E+02
7.2000000000E-02	3.3535000000E+02
7.4000000000E-02	3.3705000000E+02
7.6000000000E-02	3.3872000000E+02
7.8000000000E-02	3.4036000000E+02
8.0000000000E-02	3.4197000000E+02
8.2000000000E-02	3.4355000000E+02
8.4000000000E-02	3.4511000000E+02
8.6000000000E-02	3.4664000000E+02
8.8000000000E-02	3.4815000000E+02
9.0000000000E-02	3.4964000000E+02
9.2000000000E-02	3.5110000000E+02
9.4000000000E-02	3.5254000000E+02
9.6000000000E-02	3.5395000000E+02
9.8000000000E-02	3.5535000000E+02
1.0000000000E-01	3.5673000000E+02
1.0200000000E-01	3.5809000000E+02
1.0400000000E-01	3.5943000000E+02
1.0600000000E-01	3.6075000000E+02
1.0800000000E-01	3.6206000000E+02
1.1000000000E-01	3.6335000000E+02
1.1200000000E-01	3.6462000000E+02

1.1400000000E-01	3.6587000000E+02
1.1600000000E-01	3.6711000000E+02
1.1800000000E-01	3.6834000000E+02
1.2000000000E-01	3.6955000000E+02
1.2200000000E-01	3.7075000000E+02
1.2400000000E-01	3.7193000000E+02
1.2600000000E-01	3.7310000000E+02
1.2800000000E-01	3.7425000000E+02
1.3000000000E-01	3.7539000000E+02
1.3200000000E-01	3.7652000000E+02
1.3400000000E-01	3.7764000000E+02
1.3600000000E-01	3.7875000000E+02
1.3800000000E-01	3.7984000000E+02
1.4000000000E-01	3.8092000000E+02
1.4200000000E-01	3.8199000000E+02
1.4400000000E-01	3.8306000000E+02
1.4600000000E-01	3.8411000000E+02
1.4800000000E-01	3.8515000000E+02
1.5000000000E-01	3.8617000000E+02
1.5200000000E-01	3.8719000000E+02
1.5400000000E-01	3.8820000000E+02
1.5600000000E-01	3.8920000000E+02
1.5800000000E-01	3.9020000000E+02
1.6000000000E-01	3.9118000000E+02
1.6200000000E-01	3.9215000000E+02
1.6400000000E-01	3.9311000000E+02
1.6600000000E-01	3.9407000000E+02
1.6800000000E-01	3.9502000000E+02
1.7000000000E-01	3.9596000000E+02
1.7200000000E-01	3.9689000000E+02
1.7400000000E-01	3.9781000000E+02
1.7600000000E-01	3.9873000000E+02
1.7800000000E-01	3.9963000000E+02
1.8000000000E-01	4.0053000000E+02
1.8200000000E-01	4.0143000000E+02
1.8400000000E-01	4.0231000000E+02
1.8600000000E-01	4.0319000000E+02

1.8800000000E-01	4.0406000000E+02
1.9000000000E-01	4.0493000000E+02
1.9200000000E-01	4.0579000000E+02
1.9400000000E-01	4.0664000000E+02
1.9600000000E-01	4.0748000000E+02
1.9800000000E-01	4.0832000000E+02
2.0000000000E-01	4.0916000000E+02
2.0200000000E-01	4.0998000000E+02
2.0400000000E-01	4.1080000000E+02
2.0600000000E-01	4.1162000000E+02
2.0800000000E-01	4.1243000000E+02
2.1000000000E-01	4.1323000000E+02
2.1200000000E-01	4.1403000000E+02
2.1400000000E-01	4.1482000000E+02
2.1600000000E-01	4.1560000000E+02
2.1800000000E-01	4.1639000000E+02
2.2000000000E-01	4.1716000000E+02
2.2200000000E-01	4.1793000000E+02
2.2400000000E-01	4.1870000000E+02
2.2600000000E-01	4.1946000000E+02
2.2800000000E-01	4.2021000000E+02
2.3000000000E-01	4.2096000000E+02
2.3200000000E-01	4.2171000000E+02
2.3400000000E-01	4.2245000000E+02
2.3600000000E-01	4.2318000000E+02
2.3800000000E-01	4.2391000000E+02
2.4000000000E-01	4.2464000000E+02
2.4200000000E-01	4.2536000000E+02
2.4400000000E-01	4.2608000000E+02
2.4600000000E-01	4.2679000000E+02
2.4800000000E-01	4.2750000000E+02
2.5000000000E-01	4.2821000000E+02
2.5200000000E-01	4.2891000000E+02
2.5400000000E-01	4.2960000000E+02
2.5600000000E-01	4.3030000000E+02
2.5800000000E-01	4.3098000000E+02
2.6000000000E-01	4.3167000000E+02

2.6200000000E-01	4.3235000000E+02
2.6400000000E-01	4.3303000000E+02
2.6600000000E-01	4.3370000000E+02
2.6800000000E-01	4.3437000000E+02
2.7000000000E-01	4.3503000000E+02
2.7200000000E-01	4.3569000000E+02
2.7400000000E-01	4.3635000000E+02
2.7600000000E-01	4.3701000000E+02
2.7800000000E-01	4.3766000000E+02
2.8000000000E-01	4.3830000000E+02
2.8200000000E-01	4.3895000000E+02
2.8400000000E-01	4.3959000000E+02
2.8600000000E-01	4.4022000000E+02
2.8800000000E-01	4.4086000000E+02
2.9000000000E-01	4.4149000000E+02
2.9200000000E-01	4.4211000000E+02
2.9400000000E-01	4.4274000000E+02
2.9600000000E-01	4.4336000000E+02
2.9800000000E-01	4.4397000000E+02
3.0000000000E-01	4.4459000000E+02
3.0200000000E-01	4.4520000000E+02
3.0400000000E-01	4.4581000000E+02
3.0600000000E-01	4.4641000000E+02
3.0800000000E-01	4.4701000000E+02
3.1000000000E-01	4.4761000000E+02
3.1200000000E-01	4.4821000000E+02
3.1400000000E-01	4.4880000000E+02
3.1600000000E-01	4.4939000000E+02
3.1800000000E-01	4.4998000000E+02
3.2000000000E-01	4.5057000000E+02
3.2200000000E-01	4.5115000000E+02
3.2400000000E-01	4.5173000000E+02
3.2600000000E-01	4.5230000000E+02
3.2800000000E-01	4.5288000000E+02
3.3000000000E-01	4.5345000000E+02
3.3200000000E-01	4.5402000000E+02
3.3400000000E-01	4.5458000000E+02

3.3600000000E-01	4.5515000000E+02
3.3800000000E-01	4.5571000000E+02
3.4000000000E-01	4.5627000000E+02
3.4200000000E-01	4.5682000000E+02
3.4400000000E-01	4.5738000000E+02
3.4600000000E-01	4.5793000000E+02
3.4800000000E-01	4.5848000000E+02
3.5000000000E-01	4.5902000000E+02
3.5200000000E-01	4.5957000000E+02
3.5400000000E-01	4.6011000000E+02
3.5600000000E-01	4.6065000000E+02
3.5800000000E-01	4.6118000000E+02
3.6000000000E-01	4.6172000000E+02
3.6200000000E-01	4.6225000000E+02
3.6400000000E-01	4.6278000000E+02
3.6600000000E-01	4.6331000000E+02
3.6800000000E-01	4.6384000000E+02
3.7000000000E-01	4.6436000000E+02
3.7200000000E-01	4.6488000000E+02
3.7400000000E-01	4.6540000000E+02
3.7600000000E-01	4.6592000000E+02
3.7800000000E-01	4.6643000000E+02
3.8000000000E-01	4.6695000000E+02
3.8200000000E-01	4.6746000000E+02
3.8400000000E-01	4.6797000000E+02
3.8600000000E-01	4.6847000000E+02
3.8800000000E-01	4.6898000000E+02
3.9000000000E-01	4.6948000000E+02
3.9200000000E-01	4.6998000000E+02
3.9400000000E-01	4.7048000000E+02
3.9600000000E-01	4.7098000000E+02
3.9800000000E-01	4.7147000000E+02
4.0000000000E-01	4.7197000000E+02
4.0200000000E-01	4.7246000000E+02
4.0400000000E-01	4.7295000000E+02
4.0600000000E-01	4.7344000000E+02
4.0800000000E-01	4.7392000000E+02

4.1000000000E-01	4.7441000000E+02
4.1200000000E-01	4.7489000000E+02
4.1400000000E-01	4.7537000000E+02
4.1600000000E-01	4.7585000000E+02
4.1800000000E-01	4.7633000000E+02
4.2000000000E-01	4.7680000000E+02
4.2200000000E-01	4.7727000000E+02
4.2400000000E-01	4.7775000000E+02
4.2600000000E-01	4.7822000000E+02
4.2800000000E-01	4.7869000000E+02
4.3000000000E-01	4.7915000000E+02
4.3200000000E-01	4.7962000000E+02
4.3400000000E-01	4.8008000000E+02
4.3600000000E-01	4.8054000000E+02
4.3800000000E-01	4.8100000000E+02
4.4000000000E-01	4.8146000000E+02
4.4200000000E-01	4.8192000000E+02
4.4400000000E-01	4.8237000000E+02
4.4600000000E-01	4.8283000000E+02
4.4800000000E-01	4.8328000000E+02
4.5000000000E-01	4.8373000000E+02
4.5200000000E-01	4.8418000000E+02
4.5400000000E-01	4.8463000000E+02
4.5600000000E-01	4.8508000000E+02
4.5800000000E-01	4.8552000000E+02
4.6000000000E-01	4.8596000000E+02
4.6200000000E-01	4.8641000000E+02
4.6400000000E-01	4.8685000000E+02
4.6600000000E-01	4.8729000000E+02
4.6800000000E-01	4.8772000000E+02
4.7000000000E-01	4.8816000000E+02
4.7200000000E-01	4.8859000000E+02
4.7400000000E-01	4.8903000000E+02
4.7600000000E-01	4.8946000000E+02
4.7800000000E-01	4.8989000000E+02
4.8000000000E-01	4.9032000000E+02
4.8200000000E-01	4.9075000000E+02

```
    4.8400000000E-01    4.9117000000E+02
    4.8600000000E-01    4.9160000000E+02
    4.8800000000E-01    4.9202000000E+02
    4.9000000000E-01    4.9244000000E+02
    4.9200000000E-01    4.9287000000E+02
    4.9400000000E-01    4.9329000000E+02
    4.9600000000E-01    4.9370000000E+02
    4.9800000000E-01    4.9412000000E+02
    5.0000000000E-01    4.9454000000E+02
*DEFINE_CURVE
$VELOCITY OF 60_punch
$    LCID      SIDR      SCLA      SCLO      OFFA      OFFO    DATTYP
        23         0
$                A1                  O1
    0.0000000000E+00    0.0000000000E+00
    2.8926825769E-02    0.0000000000E+00
*DEFINE_CURVE
$VELOCITY OF 60_binder
$    LCID      SIDR      SCLA      SCLO      OFFA      OFFO    DATTYP
        24         0
$                A1                  O1
    0.0000000000E+00    0.0000000000E+00
    5.0000000000E-05    1.2311659405E+01
    1.0000000000E-04    4.8943483705E+01
    1.5000000000E-04    1.0899347581E+02
    2.0000000000E-04    1.9098300563E+02
    2.5000000000E-04    2.9289321881E+02
    3.0000000000E-04    4.1221474771E+02
    3.5000000000E-04    5.4600950026E+02
    4.0000000000E-04    6.9098300563E+02
    4.5000000000E-04    8.4356553496E+02
    5.0000000000E-04    1.0000000000E+03
    5.5000000000E-04    1.1564344650E+03
    6.0000000000E-04    1.3090169944E+03
    6.5000000000E-04    1.4539904997E+03
    7.0000000000E-04    1.5877852523E+03
    7.5000000000E-04    1.7071067812E+03
```

```
    8.0000000000E-04    1.8090169944E+03
    8.5000000000E-04    1.8910065242E+03
    9.0000000000E-04    1.9510565163E+03
    9.5000000000E-04    1.9876883406E+03
    1.0000000000E-03    2.0000000000E+03
    2.7926825769E-02    2.0000000000E+03
    2.7976825769E-02    1.9876883406E+03
    2.8026825769E-02    1.9510565163E+03
    2.8076825769E-02    1.8910065242E+03
    2.8126825769E-02    1.8090169944E+03
    2.8176825769E-02    1.7071067812E+03
    2.8226825769E-02    1.5877852523E+03
    2.8276825769E-02    1.4539904997E+03
    2.8326825769E-02    1.3090169944E+03
    2.8376825769E-02    1.1564344650E+03
    2.8426825769E-02    1.0000000000E+03
    2.8476825769E-02    8.4356553496E+02
    2.8526825769E-02    6.9098300563E+02
    2.8576825769E-02    5.4600950026E+02
    2.8626825769E-02    4.1221474771E+02
    2.8676825769E-02    2.9289321881E+02
    2.8726825769E-02    1.9098300563E+02
    2.8776825769E-02    1.0899347581E+02
    2.8826825769E-02    4.8943483705E+01
    2.8876825769E-02    1.2311659405E+01
    2.8926825769E-02    0.0000000000E+00
*DEFINE_CURVE
$VELOCITY OF 60_punch
$     LCID      SIDR      SCLA      SCLO      OFFA      OFFO    DATTYP
        25         0
$                   A1                  O1
    0.0000000000E+00    0.0000000000E+00
    5.0000000000E-05    1.2311659405E+01
    1.0000000000E-04    4.8943483705E+01
    1.5000000000E-04    1.0899347581E+02
    2.0000000000E-04    1.9098300563E+02
    2.5000000000E-04    2.9289321881E+02
```

3.0000000000E-04	4.1221474771E+02
3.5000000000E-04	5.4600950026E+02
4.0000000000E-04	6.9098300563E+02
4.5000000000E-04	8.4356553496E+02
5.0000000000E-04	1.0000000000E+03
5.5000000000E-04	1.1564344650E+03
6.0000000000E-04	1.3090169944E+03
6.5000000000E-04	1.4539904997E+03
7.0000000000E-04	1.5877852523E+03
7.5000000000E-04	1.7071067812E+03
8.0000000000E-04	1.8090169944E+03
8.5000000000E-04	1.8910065242E+03
9.0000000000E-04	1.9510565163E+03
9.5000000000E-04	1.9876883406E+03
1.0000000000E-03	2.0000000000E+03
3.7618361932E-02	2.0000000000E+03
3.7668361932E-02	1.9876883406E+03
3.7718361932E-02	1.9510565163E+03
3.7768361932E-02	1.8910065242E+03
3.7818361932E-02	1.8090169944E+03
3.7868361932E-02	1.7071067812E+03
3.7918361932E-02	1.5877852523E+03
3.7968361932E-02	1.4539904997E+03
3.8018361932E-02	1.3090169944E+03
3.8068361932E-02	1.1564344650E+03
3.8118361932E-02	1.0000000000E+03
3.8168361932E-02	8.4356553496E+02
3.8218361932E-02	6.9098300563E+02
3.8268361932E-02	5.4600950026E+02
3.8318361932E-02	4.1221474771E+02
3.8368361932E-02	2.9289321881E+02
3.8418361932E-02	1.9098300563E+02
3.8468361932E-02	1.0899347581E+02
3.8518361932E-02	4.8943483705E+01
3.8568361932E-02	1.2311659405E+01
3.8618361932E-02	0.0000000000E+00
3.9618361932E-02	0.0000000000E+00

```
*DEFINE_CURVE
$FORCE OF 60_binder
$    LCID      SIDR      SCLA      SCLO      OFFA      OFFO    DATTYP
       26         0
$                A1                  O1
   2.8926825769E-02    2.0000000000E+05
   6.8545187701E-02    2.0000000000E+05
*DEFINE_CURVE
$UPPER BOUND FOR DISPLACEMENT OF 60_binder
$    LCID      SIDR      SCLA      SCLO      OFFA      OFFO    DATTYP
       27         0
$                A1                  O1
   2.8926825769E-02    5.5853651538E+01
   6.8545187701E-02    5.5853651538E+01
$---+----1----+----2----+----3----+----4----+----5----+----6----+----7----+----8
$
$                  (8) MISCELLANEOUS
$
$---+----1----+----2----+----3----+----4----+----5----+----6----+----7----+----8
*DEFINE_VECTOR
$R.B.STOPPER DIRECTION OF 60_binder
$      VID        XT        YT        ZT        XH        YH        ZH
        3       0.0       0.0       0.0       0.0       0.0      -1.0
$---+----1----+----2----+----3----+----4----+----5----+----6----+----7----+----8
$
$                  (9) MODEL DATA
$
$---+----1----+----2----+----3----+----4----+----5----+----6----+----7----+----8
*DEFINE_TRANSFORMATION
$   TRANID
        4
$   OPTION        A1        A2        A3        A4        A5        A6        A7
   TRANSL     -93.0       0.0       0.0
*INCLUDE_TRANSFORM
$result from previous case
Simulation_2_mod_op50.dynain
$   IDNOFF    IDEOFF    IDPOFF    IDMOFF    IDSOFF    IDFOFF    IDDOFF
```

```
$   IDROFF

$   FCTMAS    FCTTIM    FCTLEN    FCTTEM   INCOUT1

$   TRANID
        4
$
*INCLUDE
Simulation_2_mod_op60.mod
$
$---+----1----+----2----+----3----+----4----+----5----+----6----+----7----+----8
*END
```

Appendix D: Input deck continuum model for HR190

```
$ ETA/DYNAFORM : LS-DYNA(971R5+) INPUT DECK
$ DATE : Nov 03, 2015 at 13:45:10
$ VERSION : eta/DYNAFORM 5.9.2, built on Aug 11 2014
$ EXPORTER : AUTO-SETUP
$
$ VIEWING INFORMATION
$  -1076.59118 -409.940582 -21.8726501 305.0237732
$  0.947067678 0.320217997 -0.02287112
$  -0.13724127 0.468235135 0.872880757
$    0.2902233 -0.82351750 0.487431258
$
$ UNIT SYSTEM : MM, TON, SEC, N
$
$ SIMULATION  : SHEET FORMING
$ RCMD-SOLVER : SINGLE
$
$---+----1----+----2----+----3----+----4----+----5----+----6----+----7----+----8
$
*KEYWORD_JOBID
Simulation_2_mod
$
$---+----1----+----2----+----3----+----4----+----5----+----6----+----7----+----8
$
$                  (1) TITLE CARD
$
$---+----1----+----2----+----3----+----4----+----5----+----6----+----7----+----8
*TITLE
untitled
$---+----1----+----2----+----3----+----4----+----5----+----6----+----7----+----8
$
$                  (2) DEFINE PARAMETERS
$
$---+----1----+----2----+----3----+----4----+----5----+----6----+----7----+----8
*PARAMETER
$    PRMR1      VAL1     PRMR2      VAL2     PRMR3      VAL3     PRMR4      VAL4
  R SCALEF       1.0
```

```
$---+----1----+----2----+----3----+----4----+----5----+----6----+----7----+----8
$
$                  (3) CONTROL CARDS
$
$---+----1----+----2----+----3----+----4----+----5----+----6----+----7----+----8
*CONTROL_TERMINATION
$   ENDTIM    ENDCYC     DTMIN    ENDNEG    ENDMAS
0.02876991        0                     0.0
*CONTROL_TIMESTEP
$   DTINIT    TSSFAC      ISDO    TSLIMT     DT2MS      LCTM     ERODE     MS1ST
       0.0       0.9         0       0.0  -3.7E-07
$   DT2MSF   DT2MSLC     IMSCL
                   0
*CONTROL_RIGID
$      LMF      JNTF    ORTHMD     PARTM    SPARSE    METALF
                                               1
*CONTROL_HOURGLASS
$      IHQ        QH
         5       0.1
*CONTROL_BULK_VISCOSITY
$       Q1        Q2      TYPE
       1.5      0.06        -2
*CONTROL_SHELL
$   WRPANG     ESORT     IRNXX    ISTUPD    THEORY       BWC     MITER      PROJ
      20.0         1        -1         1         2         2         1         0
$  ROTASCL    INTGRD    LAMSHT    CSTYP6    TSHELL    NFAIL1    NFAIL4

$  PSSTUPD    IRQUAD

$   NFAIL1    NFAIL4   PSNFAIL    KEEPCS     DELFR
         1         1
*CONTROL_SOLID
$    ESORT    FMATRX   NIPTETS    SWLOCL
         1         0         4         2
*CONTROL_CONTACT
$   SLSFAC    RWPNAL    ISLCHK    SHLTHK    PENOPT    THKCHG     ORIEN
      0.08       0.0         2         1         4         0         1
```

```
$  USRSTR   USRFAC    NSBCS   INTERM    XPENE    SSTHK    ECDT  TIEDPRJ
        0        0       10        0      1.0        0
*CONTROL_ENERGY
$    HGEN     RWEN   SLNTEN    RYLEN
        2        1        2        1
*CONTROL_OUTPUT
$   NPOPT   NEECHO   NREFUP   IACCOP    OPIFS   IPNINT   IKEDIT
        1        0        0        0      0.0        0      100
*CONTROL_PARALLEL
$    NCPU   NUMRHS    CONST
        1        0        2
*CONTROL_ACCURACY
$     OSU      INN
        0        1
*INTERFACE_SPRINGBACK_LSDYNA
$    PSID     NSHV
        1      100
*CONTROL_MPP_IO_NODUMP
$---+----1----+----2----+----3----+----4----+----5----+----6----+----7----+----8
$*DATABASE_OPTION
$      DT    BINARY
$OPTION : SECFORC RWFORC NODOUT ELOUT  GLSTAT
$         DEFORC  MATSUM NCFORC RCFORC DEFGEO
$         SPCFORC SWFORC ABSTAT NODFOR BNDOUT
$         RBDOUT  GCEOUT SLEOUT MPGS   SBTOUT
$         JNTFORC AVSFLT MOVIE
*DATABASE_RCFORC
 2.877E-05
*DATABASE_MATSUM
 2.877E-05
*DATABASE_GLSTAT
 2.877E-05
*DATABASE_SLEOUT
 2.877E-05
*DATABASE_RBDOUT
 2.877E-05
*DATABASE_BNDOUT
```

```
 2.877E-05
*DATABASE_ABSTAT
 2.877E-05
$---+----1----+----2----+----3----+----4----+----5----+----6----+----7----+----8
*DATABASE_BINARY_D3PLOT
$  DT/CYCL      LCDT      BEAM
             1
*DATABASE_EXTENT_BINARY
$    NEIPH     NEIPS    MAXINT    STRFLG    SIGFLG    EPSFLG    RLTFLG    ENGFLG
         0         0         7         1
$   CMPFLG    IEVERP    BEAMIP     DCOMP      SHGE     STSSZ
             1                   2
$---+----1----+----2----+----3----+----4----+----5----+----6----+----7----+----8
$
$                    (4) DEFINE BLANK
$
$---+----1----+----2----+----3----+----4----+----5----+----6----+----7----+----8
*SET_PART_LIST
$SET_PART_NAME: BLANK
$      SID       DA1       DA2       DA3       DA4
         1
$     PID1      PID2      PID3      PID4      PID5      PID6      PID7      PID8
       130
*PART
$HEADING
 PART PID =      130 PART NAME :BLANK130
$      PID     SECID       MID     EOSID      HGID      GRAV    ADPOPT      TMID
       130         1         1
*MAT_ANISOTROPIC_VISCOPLASTIC
$MATERIAL NAME:HRDQSK_MAT103
$      MID        RO         E        PR      SIGY      FLAG      LCSS     ALPHA
         1  7.83E-09  2.07E+05      0.28     224.4       1.0         2       0.5
$      QR1       CR1       QR2       CR2       QX1       CX1       QX2       CX2

$       VK        VM  R00 or F  R45 or G  R90 or H         L         M         N
       0.0       0.0  0.290688    0.3663    0.6337       1.5   1.21543   1.21543
$     AOPT      FAIL    NUMINT      MACF
```

```
       2.0       0.0       0.0         1
$       XP        YP        ZP        A1        A2        A3
                                 1.0       0.0       0.0
$       V1        V2        V3        D1        D2        D3      BETA
                                 0.0       1.0       0.0
*SECTION_SOLID
$    SECID    ELFORM       AET
         1         1
$---+----1----+----2----+----3----+----4----+----5----+----6----+----7----+----8
$
$                    (5) DEFINE TOOLS
$
$---+----1----+----2----+----3----+----4----+----5----+----6----+----7----+----8
$---+----1----+----2----+----3----+----4----+----5----+----6----+----7----+----8
$                    TOOL < die >
$---+----1----+----2----+----3----+----4----+----5----+----6----+----7----+----8
*SET_PART_LIST
$SET_PART_NAME: die
$      SID       DA1       DA2       DA3       DA4
        14
$     PID1      PID2      PID3      PID4      PID5      PID6      PID7      PID8
        88
*PART
$HEADING
 PART PID =        88 PART NAME :DIE00004
$      PID     SECID       MID     EOSID      HGID      GRAV    ADPOPT      TMID
        88         2         2
*MAT_RIGID
$      MID        RO         E        PR         N    COUPLE         M     ALIAS
         2  7.83E-09  2.07E+05      0.28
$      CMO      CON1      CON2
         1         7         7
$LCO or A1        A2        A3        V1        V2        V3

*SECTION_SHELL
$    SECID    ELFORM      SHRF       NIP     PROPT   QR/IRID     ICOMP     SETYP
         2         2       1.0       3.0       0.0
```

```
$      T1       T2       T3       T4     NLOC
      1.0      1.0      1.0      1.0
*CONTACT_FORMING_ONE_WAY_SURFACE_TO_SURFACE_ID
$     CID  CONTACT INTERFACE TITLE
        1  BLANK/die
$    SSID     MSID    SSTYP    MSTYP   SBOXID   MBOXID      SPR      MPR
        1       14        2        2                          1        1
$      FS       FD       DC       VC      VDC   PENCHK       BT       DT
    0.125      0.0      0.0      0.0     20.0        0      0.0    1E+20
$     SFS      SFM      SST      MST     SFST     SFMT      FSF      VSF
      0.0      0.0      0.0      0.0
$    SOFT   SOFSCL   LCIDAB   MAXPAR   PENTOL    DEPTH    BSORT   FRCFRQ
        0
$  PENMAX   THKOPT   SHLTHK    SNLOG     ISYM    I2D3D   SLDTHK   SLDSTF
                              1
$    IGAP   IGNORE   DPRFAC   DTSTIF                     FLANGL
        1
$---+----1----+----2----+----3----+----4----+----5----+----6----+----7----+----8
$                  TOOL < punch >
$---+----1----+----2----+----3----+----4----+----5----+----6----+----7----+----8
*SET_PART_LIST
$SET_PART_NAME: punch
$     SID      DA1      DA2      DA3      DA4
       15
$    PID1     PID2     PID3     PID4     PID5     PID6     PID7     PID8
      126
*PART
$HEADING
 PART PID =      126 PART NAME :FLANGE
$     PID    SECID      MID    EOSID     HGID     GRAV   ADPOPT     TMID
      126        3        3
*MAT_RIGID
$     MID       RO        E       PR        N   COUPLE        M    ALIAS
        3  7.83E-09  2.07E+05     0.28
$     CMO     CON1     CON2
        1        4        7
$LCO or A1       A2       A3       V1       V2       V3
```

```
*SECTION_SHELL
$   SECID   ELFORM    SHRF     NIP    PROPT  QR/IRID   ICOMP    SETYP
       3       2      1.0      3.0      0.0
$      T1       T2       T3       T4     NLOC
      1.0      1.0      1.0      1.0
*CONTACT_FORMING_ONE_WAY_SURFACE_TO_SURFACE_ID
$     CID  CONTACT INTERFACE TITLE
       2  BLANK/punch
$    SSID     MSID    SSTYP    MSTYP   SBOXID   MBOXID      SPR      MPR
       1       15        2        2                          1        1
$      FS       FD       DC       VC      VDC   PENCHK       BT       DT
    0.125      0.0      0.0      0.0     20.0        0      0.0    1E+20
$     SFS      SFM      SST      MST     SFST     SFMT      FSF      VSF
      0.0      0.0      0.0      0.0
$    SOFT   SOFSCL   LCIDAB   MAXPAR   PENTOL    DEPTH    BSORT   FRCFRQ
       0
$  PENMAX   THKOPT   SHLTHK    SNLOG     ISYM    I2D3D   SLDTHK   SLDSTF
                          1
$    IGAP   IGNORE   DPRFAC   DTSTIF                     FLANGL
       1
$---+----1----+----2----+----3----+----4----+----5----+----6----+----7----+----8
$                 TOOL < binder >
$---+----1----+----2----+----3----+----4----+----5----+----6----+----7----+----8
*SET_PART_LIST
$SET_PART_NAME: binder
$     SID      DA1      DA2      DA3      DA4
      16
$    PID1     PID2     PID3     PID4     PID5     PID6     PID7     PID8
     144
*PART
$HEADING
 PART PID =      144 PART NAME :BLK_HLD
$     PID    SECID      MID    EOSID     HGID     GRAV   ADPOPT     TMID
     144        4        4
*MAT_RIGID
$     MID       RO        E       PR        N   COUPLE        M    ALIAS
```

```
         4  7.83E-09  2.07E+05      0.28
$      CMO      CON1      CON2
         1         4         7
$LCO or A1        A2        A3        V1        V2        V3

*SECTION_SHELL
$    SECID    ELFORM      SHRF       NIP     PROPT   QR/IRID     ICOMP     SETYP
         4         2       1.0       3.0       0.0
$       T1        T2        T3        T4      NLOC
       1.0       1.0       1.0       1.0
*CONTACT_FORMING_ONE_WAY_SURFACE_TO_SURFACE_ID
$      CID  CONTACT INTERFACE TITLE
         3  BLANK/binder
$     SSID      MSID     SSTYP     MSTYP    SBOXID    MBOXID       SPR       MPR
         1        16         2         2                             1         1
$       FS        FD        DC        VC       VDC    PENCHK        BT        DT
     0.125       0.0       0.0       0.0      20.0         0       0.0     1E+20
$      SFS       SFM       SST       MST      SFST      SFMT       FSF       VSF
       0.0       0.0       0.0       0.0
$     SOFT    SOFSCL    LCIDAB    MAXPAR    PENTOL     DEPTH     BSORT    FRCFRQ
         0
$   PENMAX    THKOPT    SHLTHK     SNLOG      ISYM     I2D3D    SLDTHK    SLDSTF
                             1
$     IGAP    IGNORE    DPRFAC    DTSTIF                        FLANGL
         1
$---+----1----+----2----+----3----+----4----+----5----+----6----+----7----+----8
$
$                   (6) DEFINE PROCESS STEPS
$
$---+----1----+----2----+----3----+----4----+----5----+----6----+----7----+----8
$---+----1----+----2----+----3----+----4----+----5----+----6----+----7----+----8
$                   STEP < closing >
$---+----1----+----2----+----3----+----4----+----5----+----6----+----7----+----8
$die : stationary
$punch : stationary
*BOUNDARY_PRESCRIBED_MOTION_RIGID
$   typeID       DOF       VAD      LCID        SF       VID     DEATH     BIRTH
```

```
     126         3         0         3      -1.0         00.00766154       0.0
$binder : velocity
*BOUNDARY_PRESCRIBED_MOTION_RIGID
$   typeID       DOF       VAD      LCID        SF       VID     DEATH     BIRTH
     144         3         0         4      -1.0         00.00766154       0.0
$---+----1----+----2----+----3----+----4----+----5----+----6----+----7----+----8
$                  STEP < drawing >
$---+----1----+----2----+----3----+----4----+----5----+----6----+----7----+----8
$die : stationary
$punch : velocity
*BOUNDARY_PRESCRIBED_MOTION_RIGID
$   typeID       DOF       VAD      LCID        SF       VID     DEATH     BIRTH
     126         3         0         5      -1.0         00.028769910.00766154
$binder : force
*LOAD_RIGID_BODY
$      PID       DOF      LCID        SF       CID        M1        M2        M3
     144         3         6      -1.0         0
*CONSTRAINED_RIGID_BODY_STOPPERS
$      PID     LCMAX     LCMIN    PSIDMX    PSIDMN    LCVMNX       DIR       VID
     144        -7         0         0         0         0         4         1
$       TB        TD
0.007661540.02976991
$---+----1----+----2----+----3----+----4----+----5----+----6----+----7----+----8
$
$                  (7) DEFINE CURVES
$
$---+----1----+----2----+----3----+----4----+----5----+----6----+----7----+----8
*DEFINE_CURVE
$D3PLOT
$     LCID      SIDR      SCLA      SCLO      OFFA      OFFO    DATTYP
         1         0
$                A1                  O1
   0.0000000000E+00    1.5323090842E-03
   1.5323090842E-03    1.5323090842E-03
   3.0646181683E-03    1.5323090842E-03
   4.5969272525E-03    1.5323090842E-03
   6.1292363367E-03    1.5323090842E-03
```

```
   7.6615454208E-03    3.1083653654E-03
   1.0769910786E-02    4.9999987510E-03
   1.5769909537E-02    2.4999993755E-03
   1.8269908913E-02    2.4999993755E-03
   2.0769908288E-02    2.4999993755E-03
   2.3269907664E-02    2.4999993755E-03
   2.5769907039E-02    1.0000143287E-03
   2.6769921368E-02    9.9999610556E-04
   2.7769917473E-02    1.0000000000E-03
   2.8769917473E-02    1.0000000000E-03
*DEFINE_CURVE
$SSC
$     LCID      SIDR      SCLA      SCLO      OFFA      OFFO    DATTYP
        2         0
$                 A1                  O1
   0.0000000000E+00    2.2098000000E+02
   2.0000000000E-03    2.2838000000E+02
   4.0000000000E-03    2.3499000000E+02
   6.0000000000E-03    2.4099000000E+02
   8.0000000000E-03    2.4649000000E+02
   1.0000000000E-02    2.5157000000E+02
   1.2000000000E-02    2.5630000000E+02
   1.4000000000E-02    2.6074000000E+02
   1.6000000000E-02    2.6491000000E+02
   1.8000000000E-02    2.6886000000E+02
   2.0000000000E-02    2.7261000000E+02
   2.2000000000E-02    2.7618000000E+02
   2.4000000000E-02    2.7958000000E+02
   2.6000000000E-02    2.8284000000E+02
   2.8000000000E-02    2.8597000000E+02
   3.0000000000E-02    2.8898000000E+02
   3.2000000000E-02    2.9188000000E+02
   3.4000000000E-02    2.9468000000E+02
   3.6000000000E-02    2.9738000000E+02
   3.8000000000E-02    3.0000000000E+02
   4.0000000000E-02    3.0254000000E+02
   4.2000000000E-02    3.0500000000E+02
```

4.4000000000E-02	3.0739000000E+02
4.6000000000E-02	3.0971000000E+02
4.8000000000E-02	3.1198000000E+02
5.0000000000E-02	3.1418000000E+02
5.2000000000E-02	3.1633000000E+02
5.4000000000E-02	3.1843000000E+02
5.6000000000E-02	3.2047000000E+02
5.8000000000E-02	3.2248000000E+02
6.0000000000E-02	3.2443000000E+02
6.2000000000E-02	3.2635000000E+02
6.4000000000E-02	3.2822000000E+02
6.6000000000E-02	3.3006000000E+02
6.8000000000E-02	3.3186000000E+02
7.0000000000E-02	3.3362000000E+02
7.2000000000E-02	3.3535000000E+02
7.4000000000E-02	3.3705000000E+02
7.6000000000E-02	3.3872000000E+02
7.8000000000E-02	3.4036000000E+02
8.0000000000E-02	3.4197000000E+02
8.2000000000E-02	3.4355000000E+02
8.4000000000E-02	3.4511000000E+02
8.6000000000E-02	3.4664000000E+02
8.8000000000E-02	3.4815000000E+02
9.0000000000E-02	3.4964000000E+02
9.2000000000E-02	3.5110000000E+02
9.4000000000E-02	3.5254000000E+02
9.6000000000E-02	3.5395000000E+02
9.8000000000E-02	3.5535000000E+02
1.0000000000E-01	3.5673000000E+02
1.0200000000E-01	3.5809000000E+02
1.0400000000E-01	3.5943000000E+02
1.0600000000E-01	3.6075000000E+02
1.0800000000E-01	3.6206000000E+02
1.1000000000E-01	3.6335000000E+02
1.1200000000E-01	3.6462000000E+02
1.1400000000E-01	3.6587000000E+02
1.1600000000E-01	3.6711000000E+02

1.1800000000E-01	3.6834000000E+02
1.2000000000E-01	3.6955000000E+02
1.2200000000E-01	3.7075000000E+02
1.2400000000E-01	3.7193000000E+02
1.2600000000E-01	3.7310000000E+02
1.2800000000E-01	3.7425000000E+02
1.3000000000E-01	3.7539000000E+02
1.3200000000E-01	3.7652000000E+02
1.3400000000E-01	3.7764000000E+02
1.3600000000E-01	3.7875000000E+02
1.3800000000E-01	3.7984000000E+02
1.4000000000E-01	3.8092000000E+02
1.4200000000E-01	3.8199000000E+02
1.4400000000E-01	3.8306000000E+02
1.4600000000E-01	3.8411000000E+02
1.4800000000E-01	3.8515000000E+02
1.5000000000E-01	3.8617000000E+02
1.5200000000E-01	3.8719000000E+02
1.5400000000E-01	3.8820000000E+02
1.5600000000E-01	3.8920000000E+02
1.5800000000E-01	3.9020000000E+02
1.6000000000E-01	3.9118000000E+02
1.6200000000E-01	3.9215000000E+02
1.6400000000E-01	3.9311000000E+02
1.6600000000E-01	3.9407000000E+02
1.6800000000E-01	3.9502000000E+02
1.7000000000E-01	3.9596000000E+02
1.7200000000E-01	3.9689000000E+02
1.7400000000E-01	3.9781000000E+02
1.7600000000E-01	3.9873000000E+02
1.7800000000E-01	3.9963000000E+02
1.8000000000E-01	4.0053000000E+02
1.8200000000E-01	4.0143000000E+02
1.8400000000E-01	4.0231000000E+02
1.8600000000E-01	4.0319000000E+02
1.8800000000E-01	4.0406000000E+02
1.9000000000E-01	4.0493000000E+02

1.9200000000E-01	4.0579000000E+02
1.9400000000E-01	4.0664000000E+02
1.9600000000E-01	4.0748000000E+02
1.9800000000E-01	4.0832000000E+02
2.0000000000E-01	4.0916000000E+02
2.0200000000E-01	4.0998000000E+02
2.0400000000E-01	4.1080000000E+02
2.0600000000E-01	4.1162000000E+02
2.0800000000E-01	4.1243000000E+02
2.1000000000E-01	4.1323000000E+02
2.1200000000E-01	4.1403000000E+02
2.1400000000E-01	4.1482000000E+02
2.1600000000E-01	4.1560000000E+02
2.1800000000E-01	4.1639000000E+02
2.2000000000E-01	4.1716000000E+02
2.2200000000E-01	4.1793000000E+02
2.2400000000E-01	4.1870000000E+02
2.2600000000E-01	4.1946000000E+02
2.2800000000E-01	4.2021000000E+02
2.3000000000E-01	4.2096000000E+02
2.3200000000E-01	4.2171000000E+02
2.3400000000E-01	4.2245000000E+02
2.3600000000E-01	4.2318000000E+02
2.3800000000E-01	4.2391000000E+02
2.4000000000E-01	4.2464000000E+02
2.4200000000E-01	4.2536000000E+02
2.4400000000E-01	4.2608000000E+02
2.4600000000E-01	4.2679000000E+02
2.4800000000E-01	4.2750000000E+02
2.5000000000E-01	4.2821000000E+02
2.5200000000E-01	4.2891000000E+02
2.5400000000E-01	4.2960000000E+02
2.5600000000E-01	4.3030000000E+02
2.5800000000E-01	4.3098000000E+02
2.6000000000E-01	4.3167000000E+02
2.6200000000E-01	4.3235000000E+02
2.6400000000E-01	4.3303000000E+02

2.6600000000E-01	4.3370000000E+02
2.6800000000E-01	4.3437000000E+02
2.7000000000E-01	4.3503000000E+02
2.7200000000E-01	4.3569000000E+02
2.7400000000E-01	4.3635000000E+02
2.7600000000E-01	4.3701000000E+02
2.7800000000E-01	4.3766000000E+02
2.8000000000E-01	4.3830000000E+02
2.8200000000E-01	4.3895000000E+02
2.8400000000E-01	4.3959000000E+02
2.8600000000E-01	4.4022000000E+02
2.8800000000E-01	4.4086000000E+02
2.9000000000E-01	4.4149000000E+02
2.9200000000E-01	4.4211000000E+02
2.9400000000E-01	4.4274000000E+02
2.9600000000E-01	4.4336000000E+02
2.9800000000E-01	4.4397000000E+02
3.0000000000E-01	4.4459000000E+02
3.0200000000E-01	4.4520000000E+02
3.0400000000E-01	4.4581000000E+02
3.0600000000E-01	4.4641000000E+02
3.0800000000E-01	4.4701000000E+02
3.1000000000E-01	4.4761000000E+02
3.1200000000E-01	4.4821000000E+02
3.1400000000E-01	4.4880000000E+02
3.1600000000E-01	4.4939000000E+02
3.1800000000E-01	4.4998000000E+02
3.2000000000E-01	4.5057000000E+02
3.2200000000E-01	4.5115000000E+02
3.2400000000E-01	4.5173000000E+02
3.2600000000E-01	4.5230000000E+02
3.2800000000E-01	4.5288000000E+02
3.3000000000E-01	4.5345000000E+02
3.3200000000E-01	4.5402000000E+02
3.3400000000E-01	4.5458000000E+02
3.3600000000E-01	4.5515000000E+02
3.3800000000E-01	4.5571000000E+02

3.4000000000E-01	4.5627000000E+02
3.4200000000E-01	4.5682000000E+02
3.4400000000E-01	4.5738000000E+02
3.4600000000E-01	4.5793000000E+02
3.4800000000E-01	4.5848000000E+02
3.5000000000E-01	4.5902000000E+02
3.5200000000E-01	4.5957000000E+02
3.5400000000E-01	4.6011000000E+02
3.5600000000E-01	4.6065000000E+02
3.5800000000E-01	4.6118000000E+02
3.6000000000E-01	4.6172000000E+02
3.6200000000E-01	4.6225000000E+02
3.6400000000E-01	4.6278000000E+02
3.6600000000E-01	4.6331000000E+02
3.6800000000E-01	4.6384000000E+02
3.7000000000E-01	4.6436000000E+02
3.7200000000E-01	4.6488000000E+02
3.7400000000E-01	4.6540000000E+02
3.7600000000E-01	4.6592000000E+02
3.7800000000E-01	4.6643000000E+02
3.8000000000E-01	4.6695000000E+02
3.8200000000E-01	4.6746000000E+02
3.8400000000E-01	4.6797000000E+02
3.8600000000E-01	4.6847000000E+02
3.8800000000E-01	4.6898000000E+02
3.9000000000E-01	4.6948000000E+02
3.9200000000E-01	4.6998000000E+02
3.9400000000E-01	4.7048000000E+02
3.9600000000E-01	4.7098000000E+02
3.9800000000E-01	4.7147000000E+02
4.0000000000E-01	4.7197000000E+02
4.0200000000E-01	4.7246000000E+02
4.0400000000E-01	4.7295000000E+02
4.0600000000E-01	4.7344000000E+02
4.0800000000E-01	4.7392000000E+02
4.1000000000E-01	4.7441000000E+02
4.1200000000E-01	4.7489000000E+02

4.1400000000E-01	4.7537000000E+02
4.1600000000E-01	4.7585000000E+02
4.1800000000E-01	4.7633000000E+02
4.2000000000E-01	4.7680000000E+02
4.2200000000E-01	4.7727000000E+02
4.2400000000E-01	4.7775000000E+02
4.2600000000E-01	4.7822000000E+02
4.2800000000E-01	4.7869000000E+02
4.3000000000E-01	4.7915000000E+02
4.3200000000E-01	4.7962000000E+02
4.3400000000E-01	4.8008000000E+02
4.3600000000E-01	4.8054000000E+02
4.3800000000E-01	4.8100000000E+02
4.4000000000E-01	4.8146000000E+02
4.4200000000E-01	4.8192000000E+02
4.4400000000E-01	4.8237000000E+02
4.4600000000E-01	4.8283000000E+02
4.4800000000E-01	4.8328000000E+02
4.5000000000E-01	4.8373000000E+02
4.5200000000E-01	4.8418000000E+02
4.5400000000E-01	4.8463000000E+02
4.5600000000E-01	4.8508000000E+02
4.5800000000E-01	4.8552000000E+02
4.6000000000E-01	4.8596000000E+02
4.6200000000E-01	4.8641000000E+02
4.6400000000E-01	4.8685000000E+02
4.6600000000E-01	4.8729000000E+02
4.6800000000E-01	4.8772000000E+02
4.7000000000E-01	4.8816000000E+02
4.7200000000E-01	4.8859000000E+02
4.7400000000E-01	4.8903000000E+02
4.7600000000E-01	4.8946000000E+02
4.7800000000E-01	4.8989000000E+02
4.8000000000E-01	4.9032000000E+02
4.8200000000E-01	4.9075000000E+02
4.8400000000E-01	4.9117000000E+02
4.8600000000E-01	4.9160000000E+02

```
   4.8800000000E-01    4.9202000000E+02
   4.9000000000E-01    4.9244000000E+02
   4.9200000000E-01    4.9287000000E+02
   4.9400000000E-01    4.9329000000E+02
   4.9600000000E-01    4.9370000000E+02
   4.9800000000E-01    4.9412000000E+02
   5.0000000000E-01    4.9454000000E+02
*DEFINE_CURVE
$VELOCITY OF punch
$    LCID     SIDR     SCLA     SCLO     OFFA     OFFO    DATTYP
        3        0
$               A1                 O1
   0.0000000000E+00    0.0000000000E+00
   7.6615454208E-03    0.0000000000E+00
*DEFINE_CURVE
$VELOCITY OF binder
$    LCID     SIDR     SCLA     SCLO     OFFA     OFFO    DATTYP
        4        0
$               A1                 O1
   0.0000000000E+00    0.0000000000E+00
   5.0000000000E-05    1.2311659405E+01
   1.0000000000E-04    4.8943483705E+01
   1.5000000000E-04    1.0899347581E+02
   2.0000000000E-04    1.9098300563E+02
   2.5000000000E-04    2.9289321881E+02
   3.0000000000E-04    4.1221474771E+02
   3.5000000000E-04    5.4600950026E+02
   4.0000000000E-04    6.9098300563E+02
   4.5000000000E-04    8.4356553496E+02
   5.0000000000E-04    1.0000000000E+03
   5.5000000000E-04    1.1564344650E+03
   6.0000000000E-04    1.3090169944E+03
   6.5000000000E-04    1.4539904997E+03
   7.0000000000E-04    1.5877852523E+03
   7.5000000000E-04    1.7071067812E+03
   8.0000000000E-04    1.8090169944E+03
   8.5000000000E-04    1.8910065242E+03
```

```
    9.0000000000E-04    1.9510565163E+03
    9.5000000000E-04    1.9876883406E+03
    1.0000000000E-03    2.0000000000E+03
    6.6615454208E-03    2.0000000000E+03
    6.7115454208E-03    1.9876883406E+03
    6.7615454208E-03    1.9510565163E+03
    6.8115454208E-03    1.8910065242E+03
    6.8615454208E-03    1.8090169944E+03
    6.9115454208E-03    1.7071067812E+03
    6.9615454208E-03    1.5877852523E+03
    7.0115454208E-03    1.4539904997E+03
    7.0615454208E-03    1.3090169944E+03
    7.1115454208E-03    1.1564344650E+03
    7.1615454208E-03    1.0000000000E+03
    7.2115454208E-03    8.4356553496E+02
    7.2615454208E-03    6.9098300563E+02
    7.3115454208E-03    5.4600950026E+02
    7.3615454208E-03    4.1221474771E+02
    7.4115454208E-03    2.9289321881E+02
    7.4615454208E-03    1.9098300563E+02
    7.5115454208E-03    1.0899347581E+02
    7.5615454208E-03    4.8943483705E+01
    7.6115454208E-03    1.2311659405E+01
    7.6615454208E-03    0.0000000000E+00
*DEFINE_CURVE
$VELOCITY OF punch
$     LCID      SIDR      SCLA      SCLO      OFFA      OFFO    DATTYP
         5         0
$                 A1                  O1
    0.0000000000E+00    0.0000000000E+00
    5.0000000000E-05    1.2311659405E+01
    1.0000000000E-04    4.8943483705E+01
    1.5000000000E-04    1.0899347581E+02
    2.0000000000E-04    1.9098300563E+02
    2.5000000000E-04    2.9289321881E+02
    3.0000000000E-04    4.1221474771E+02
    3.5000000000E-04    5.4600950026E+02
```

```
    4.0000000000E-04    6.9098300563E+02
    4.5000000000E-04    8.4356553496E+02
    5.0000000000E-04    1.0000000000E+03
    5.5000000000E-04    1.1564344650E+03
    6.0000000000E-04    1.3090169944E+03
    6.5000000000E-04    1.4539904997E+03
    7.0000000000E-04    1.5877852523E+03
    7.5000000000E-04    1.7071067812E+03
    8.0000000000E-04    1.8090169944E+03
    8.5000000000E-04    1.8910065242E+03
    9.0000000000E-04    1.9510565163E+03
    9.5000000000E-04    1.9876883406E+03
    1.0000000000E-03    2.0000000000E+03
    2.0108372053E-02    2.0000000000E+03
    2.0158372053E-02    1.9876883406E+03
    2.0208372053E-02    1.9510565163E+03
    2.0258372053E-02    1.8910065242E+03
    2.0308372053E-02    1.8090169944E+03
    2.0358372053E-02    1.7071067812E+03
    2.0408372053E-02    1.5877852523E+03
    2.0458372053E-02    1.4539904997E+03
    2.0508372053E-02    1.3090169944E+03
    2.0558372053E-02    1.1564344650E+03
    2.0608372053E-02    1.0000000000E+03
    2.0658372053E-02    8.4356553496E+02
    2.0708372053E-02    6.9098300563E+02
    2.0758372053E-02    5.4600950026E+02
    2.0808372053E-02    4.1221474771E+02
    2.0858372053E-02    2.9289321881E+02
    2.0908372053E-02    1.9098300563E+02
    2.0958372053E-02    1.0899347581E+02
    2.1008372053E-02    4.8943483705E+01
    2.1058372053E-02    1.2311659405E+01
    2.1108372053E-02    0.0000000000E+00
    2.2108372053E-02    0.0000000000E+00
*DEFINE_CURVE
$FORCE OF binder
```

```
$    LCID     SIDR     SCLA     SCLO     OFFA     OFFO   DATTYP
        6        0
$              A1                O1
   7.6615454208E-03    2.0000000000E+05
   2.9769917473E-02    2.0000000000E+05
*DEFINE_CURVE
$UPPER BOUND FOR DISPLACEMENT OF binder
$    LCID     SIDR     SCLA     SCLO     OFFA     OFFO   DATTYP
        7        0
$              A1                O1
   7.6615454208E-03    1.3323090842E+01
   2.9769917473E-02    1.3323090842E+01
$---+----1----+----2----+----3----+----4----+----5----+----6----+----7----+----8
$
$                 (8) MISCELLANEOUS
$
$---+----1----+----2----+----3----+----4----+----5----+----6----+----7----+----8
*DEFINE_VECTOR
$R.B.STOPPER DIRECTION OF binder
$     VID       XT       YT       ZT       XH       YH       ZH
        1      0.0      0.0      0.0      0.0      0.0     -1.0
$---+----1----+----2----+----3----+----4----+----5----+----6----+----7----+----8
$                 (9) MODEL DATA
$
$---+----1----+----2----+----3----+----4----+----5----+----6----+----7----+----8
*INCLUDE
Simulation_2_mod.blk
$
*INCLUDE
Simulation_2_mod_op60.mod
$
$---+----1----+----2----+----3----+----4----+----5----+----6----+----7----+----8
${{DYNAFORM-AUTOSETUP-CMPRS1->>>DO NOT MODIFY>>>
$}}DYNAFORM-AUTOSETUP
$---+----1----+----2----+----3----+----4----+----5----+----6----+----7----+----8
$---+----1----+----2----+----3----+----4----+----5----+----6----+----7----+----8
*END
```

Appendix E: Statistical CMM raw data

Date: 2016/ 3/14

Model name: Part Model Original.ige

Operator: Admin

Meas. mode surface

Max. deviation : 1.384 mm (36)

Mean deviation : -0.002 mm

Min. deviation: -1.346 mm (46)

Best fit

Shift: 0.567 mm -0.542 mm 0.048 mm

Rot.: -0.343 ° -0.299 ° 0.502 °

Comments:

No. Meas. Probe

Mode CAD Tolerances

Dev. (X, Y, Z) Total Deviation

1 -21.998 10.373 -0.230 1.960

SurF -21.998 10.373 -0.000 -0.500 0.500

-0.000 -0.000 -0.230 -0.230 ---**+-----

2 -19.890 -18.576 0.035 1.960

SurF -19.890 -18.576 0.000 -0.500 0.500

0.000 0.000 0.035 0.035 -----+-----

3 4.354 -29.668 0.255 1.960

SurF 4.354 -29.668 0.000 -0.500 0.500

0.000 0.000 0.255 0.255 -----+***--

4 -12.324 39.745 3.714 1.962

SurF -12.307 40.382 3.537 -0.500 0.500

-0.016 -0.637 0.177 0.662 -----+--->>

5 -3.074 39.703 3.762 1.962

SurF -3.062 40.172 3.632 -0.500 0.500
-0.012 -0.469 0.130 0.487 -----+*****

6 6.808 39.602 3.814 1.962
SurF 6.817 39.943 3.719 -0.500 0.500
-0.009 -0.340 0.095 0.353 -----+****-

7 14.734 39.546 3.855 1.962
SurF 14.740 39.761 3.795 -0.500 0.500
-0.005 -0.215 0.060 0.223 -----+**---

8 23.321 39.514 3.907 1.962
SurF 23.322 39.568 3.892 -0.500 0.500
-0.001 -0.054 0.015 0.056 -----+*----

9 31.246 39.725 3.946 1.962
SurF 31.238 39.405 4.035 -0.500 0.500
0.008 0.320 -0.089 -0.332 --***+-----

10 32.635 42.402 12.331 1.962
SurF 32.618 41.731 12.518 -0.500 0.500
0.017 0.672 -0.187 -0.698 <<---+-----

11 19.338 42.340 12.263 1.962
SurF 19.330 42.025 12.351 -0.500 0.500
0.008 0.315 -0.088 -0.328 --***+-----

12 -0.379 42.349 12.161 1.962
SurF -0.376 42.468 12.128 -0.500 0.500
-0.003 -0.119 0.033 0.123 -----+*----

13 -14.118 42.352 12.090 1.962
SurF -14.107 42.776 11.972 -0.500 0.500
-0.011 -0.424 0.118 0.440 -----+****-

14 -10.430 46.276 25.127 1.962
SurF -10.428 46.338 25.109 -0.500 0.500

	-0.002	-0.062	0.017	0.065	-----+*----
15	8.336	46.287	25.239	1.962	
SurF	8.326	45.922	25.340	-0.500	0.500
	0.009	0.366	-0.102	-0.380	-****+-----
16	28.511	46.393	25.342	1.962	
SurF	28.487	45.476	25.597	-0.500	0.500
	0.023	0.917	-0.255	-0.952	<<---+-----
17	37.302	9.293	8.083	1.962	
SurF	37.302	9.293	7.000	-0.500	0.500
	-0.000	0.000	1.083	-1.083	<<---+-----
18	37.131	9.185	2.606	1.962	
SurF	36.877	9.192	3.000	-0.500	0.500
	0.254	-0.007	-0.394	-0.469	*****+-----
19	37.937	17.732	7.235	1.962	
SurF	37.096	17.753	7.000	-0.500	0.500
	0.841	-0.022	0.235	-0.873	<<---+-----
20	37.360	18.059	3.300	1.962	
SurF	37.104	18.065	3.300	-0.500	0.500
	0.256	-0.007	-0.000	-0.256	--***+-----
21	37.266	25.232	7.044	1.962	
SurF	37.287	25.207	7.000	-0.500	0.500
	-0.021	0.025	0.044	0.054	-----+*----
22	37.182	25.549	2.782	1.962	
SurF	37.288	25.546	2.774	-0.500	0.500
	-0.106	0.003	0.008	0.106	-----+*----
23	37.220	33.275	8.719	1.962	
SurF	37.494	33.268	8.719	-0.500	0.500
	-0.274	0.007	-0.000	0.274	-----+***--

24	37.248	33.233	3.808	1.962	
SurF	37.493	33.227	3.808	-0.500	0.500
	-0.245	0.006	-0.000	0.245	-----+**---
25	37.167	36.181	11.031	1.962	
SurF	37.568	36.171	11.031	-0.500	0.500
	-0.401	0.010	-0.000	0.401	-----+****-
26	37.202	38.424	10.971	1.962	
SurF	37.601	38.465	10.957	-0.500	0.500
	-0.399	-0.041	0.014	0.401	-----+****-
27	37.316	36.934	16.320	1.962	
SurF	37.588	36.927	16.320	-0.500	0.500
	-0.272	0.007	-0.000	0.272	-----+***--
28	37.194	40.278	16.221	1.962	
SurF	37.560	40.369	16.193	-0.500	0.500
	-0.367	-0.091	0.028	0.379	-----+****-
29	37.667	39.944	22.436	1.962	
SurF	37.728	39.944	22.431	-0.500	0.500
	-0.061	0.001	0.005	0.061	-----+*----
30	37.642	41.717	22.400	1.962	
SurF	37.721	41.726	22.391	-0.500	0.500
	-0.079	-0.009	0.008	0.080	-----+*----
31	38.377	41.716	25.978	1.962	
SurF	38.327	41.715	25.991	-0.500	0.500
	0.050	0.001	-0.013	-0.052	----*+-----
32	38.251	42.514	25.890	1.962	
SurF	38.279	42.527	25.879	-0.500	0.500
	-0.029	-0.013	0.011	0.034	-----+-----

33	-4.265	46.691	33.119	1.962		
SurF	-4.262	46.835	33.146	-0.500	0.500	
	-0.004	-0.144	-0.027	0.147	-----+*----	
34	15.751	46.719	33.210	1.962		
SurF	15.741	46.325	33.135	-0.500	0.500	
	0.010	0.394	0.075	-0.401	-****+-----	
35	30.454	46.789	33.285	1.962		
SurF	30.432	45.950	33.126	-0.500	0.500	
	0.022	0.839	0.159	-0.854	<<---+-----	
36	43.987	44.720	46.455	1.962		
SurF	44.022	46.080	46.713	-0.500	0.500	
	-0.035	-1.360	-0.258	1.384	-----+--->>	
37	29.653	44.547	46.393	1.962		
SurF	29.626	43.493	46.193	-0.500	0.500	
	0.027	1.054	0.200	-1.073	<<---+-----	
38	7.772	44.500	46.281	1.962		
SurF	7.760	44.053	46.196	-0.500	0.500	
	0.011	0.447	0.085	-0.455	*****+-----	
39	14.874	40.818	62.142	1.962		
SurF	14.405	40.793	62.492	-0.500	0.500	
	0.469	0.026	-0.349	0.585	-----+--->>	
40	29.157	41.850	61.809	1.962		
SurF	29.125	40.590	61.570	-0.500	0.500	
	0.032	1.260	0.239	-1.283	<<---+-----	
41	45.587	42.033	61.891	1.962		
SurF	45.615	43.122	62.098	-0.500	0.500	
	-0.028	-1.089	-0.207	1.109	-----+--->>	
42	64.367	42.294	62.002	1.962		

SurF	64.376	42.647	62.069	-0.500	0.500
	-0.009	-0.352	-0.067	0.359	-----+****-
43	65.067	36.689	94.096	1.962	
SurF	65.064	36.561	94.071	-0.500	0.500
	0.003	0.128	0.024	-0.130	----*+-----
44	49.826	36.520	94.019	1.962	
SurF	49.837	36.946	94.099	-0.500	0.500
	-0.011	-0.425	-0.081	0.433	-----+****-
45	27.738	36.304	93.906	1.962	
SurF	27.769	37.505	94.134	-0.500	0.500
	-0.031	-1.201	-0.228	1.223	-----+--->>
46	22.878	38.779	79.192	1.962	
SurF	22.844	37.457	78.942	-0.500	0.500
	0.034	1.322	0.251	-1.346	<<---+-----
47	42.478	38.965	79.277	1.962	
SurF	42.502	39.910	79.456	-0.500	0.500
	-0.024	-0.946	-0.179	0.963	-----+--->>
48	52.919	39.082	79.332	1.962	
SurF	52.934	39.646	79.439	-0.500	0.500
	-0.014	-0.564	-0.107	0.574	-----+--->>
49	67.848	39.262	79.407	1.962	
SurF	67.848	39.270	79.408	-0.500	0.500
	-0.000	-0.007	-0.001	0.008	-----+-----
50	-22.096	11.568	-0.247	1.960	
SurF	-22.096	11.568	-0.000	-0.500	0.500
	-0.000	-0.000	-0.247	-0.247	---**+-----
51	-20.621	-12.298	-0.013	1.960	
SurF	-20.621	-12.298	0.000	-0.500	0.500

	-0.000	-0.000	-0.013	-0.013	-----+-----
52	-0.955	-20.797	0.221	1.960	
SurF	-0.955	-20.797	0.000	-0.500	0.500
	0.000	0.000	0.221	0.221	-----+**---
53	20.304	-15.327	0.231	1.960	
SurF	20.304	-15.327	0.000	-0.500	0.500
	0.000	0.000	0.231	0.231	-----+**---
54	24.876	7.171	0.053	1.960	
SurF	24.876	7.171	-0.000	-0.500	0.500
	0.000	0.000	0.053	0.053	-----+*----
55	14.094	21.569	0.019	1.960	
SurF	14.094	21.569	-0.000	-0.500	0.500
	0.000	0.000	0.019	0.019	-----+-----
56	30.340	22.063	0.010	1.960	
SurF	30.340	22.063	-0.000	-0.500	0.500
	0.000	0.000	0.010	0.010	-----+-----
57	31.114	12.789	-0.038	1.960	
SurF	31.114	12.789	-0.000	-0.500	0.500
	-0.000	-0.000	-0.038	-0.038	-----+-----
58	-1.796	26.791	-0.116	1.960	
SurF	-1.796	26.791	-0.000	-0.500	0.500
	-0.000	-0.000	-0.116	-0.116	----*+-----
59	-4.339	33.042	-0.185	1.960	
SurF	-4.339	33.042	-0.000	-0.500	0.500
	-0.000	-0.000	-0.185	-0.185	---**+-----
60	-13.324	32.257	-0.303	1.960	
SurF	-13.324	32.257	-0.000	-0.500	0.500
	-0.000	-0.000	-0.303	-0.303	--***+-----

61	-12.818	26.454	-0.237	1.960	
SurF	-12.818	26.454	-0.000	-0.500	0.500
	-0.000	-0.000	-0.237	-0.237	---**+-----

62	-10.073	17.789	-0.095	1.960	
SurF	-10.073	17.789	-0.000	-0.500	0.500
	-0.000	-0.000	-0.095	-0.095	----*+-----